

# Prodromal Glutamatergic Modulation with Riluzole Impacts Glucose Homeostasis and Spatial Cognition in Alzheimer's Disease Mice

Caleigh A. Findley<sup>a,b</sup>, Samuel A. McFadden<sup>a</sup>, MaKayla F. Cox<sup>a</sup>, Lindsey N. Sime<sup>a</sup>, Mackenzie R. Peck<sup>a</sup>, Kathleen Quinn<sup>a</sup>, Andrzej Bartke<sup>c,d</sup>, Kevin N. Hascup<sup>a,b,c</sup> and Erin R. Hascup<sup>a,b,\*</sup>

<sup>a</sup>Neuroscience Institute, Dale and Deborah Smith Center for Alzheimer's Research and Treatment, Department of Neurology, Southern Illinois University School of Medicine, Springfield, IL, USA

<sup>b</sup>Departments of Pharmacology, Southern Illinois University School of Medicine, Springfield, IL, USA

<sup>c</sup>Department of Medical Microbiology, Immunology and Cell Biology, Southern Illinois University School of Medicine, Springfield, IL, USA

<sup>d</sup>Department of Internal Medicine, Southern Illinois University School of Medicine, Springfield, IL, USA

Accepted 26 April 2023

Pre-press 23 May 2023

## Abstract.

**Background:** Prior research supports a strong link between Alzheimer's disease (AD) and metabolic dysfunction that involves a multi-directional interaction between glucose, glutamatergic homeostasis, and amyloid pathology. Elevated soluble amyloid- $\beta$  (A $\beta$ ) is an early biomarker for AD-associated cognitive decline that contributes to concurrent glutamatergic and metabolic dyshomeostasis in humans and male transgenic AD mice. Yet, it remains unclear how primary time-sensitive targeting of hippocampal glutamatergic activity may impact glucose regulation in an amyloidogenic mouse model. Previous studies have illustrated increased glucose uptake and metabolism using a neuroprotective glutamate modulator (riluzole), supporting the link between glucose and glutamatergic homeostasis.

**Objective:** We hypothesized that targeting early glutamatergic hyperexcitation through riluzole treatment could aid in attenuating co-occurring metabolic and amyloidogenic pathologies with the intent of ameliorating cognitive decline.

**Methods:** We conducted an early intervention study in male and female transgenic (A $\beta$ PP/PS1) and knock-in (APP<sup>NL-F/NL-F</sup>) AD mice to assess the on- and off-treatment effects of prodromal glutamatergic modulation (2–6 months of age) on glucose homeostasis and spatial cognition through riluzole treatment.

**Results:** Results indicated a sex- and genotype-specific effect on glucose homeostasis and spatial cognition with riluzole intervention that evolved with disease progression and time since treatment.

**Conclusion:** These findings support the interconnected nature of glucose and glutamatergic homeostasis with amyloid pathology and petition for further investigation into the targeting of this relationship to improve cognitive performance.

Keywords: Alzheimer's disease, amyloid, hippocampus, insulin, learning, memory, metabolism

---

\*Correspondence to: Erin R. Hascup, Department of Neurology, Dale and Deborah Smith Center for Alzheimer's Research and Treatment, Southern Illinois University School of Medicine,

---

P.O. Box 19628, Springfield, IL 62794-9628, USA. E-mail: ehascup@siumed.edu.

## INTRODUCTION

In the United States, ~6.5 million people have been diagnosed with Alzheimer's disease (AD), almost two-thirds of whom are women [1]. AD is ranked 6th in the *Top Ten Causes of Death* by the Centers for Disease Control, amongst other related conditions such as diabetes and heart disease [2]. Evidence supports a strong epidemiological link between AD and metabolic dysfunction, such that some researchers now define AD as Type 3 Diabetes [3]. It is estimated that Type-2 Diabetes increases the risk for AD by ~65% and that ~80% of AD patients are either pre-diabetic or diabetic [4]. The association between these two diseases may result from their shared pathological mechanisms and similarities in disease-influencing factors, such as obesity, age, and diet [3].

A limited number of drugs have been approved for AD treatment, while many others have failed in clinical trials. Most AD pharmacotherapies treat the symptoms while next-generation medications remove pathologies associated with disease progression but are controversial as to their disease-modifying effects [5]. Prior work from our laboratories and others indicates the appearance of abnormalities in amyloid, glucose homeostasis, and glutamatergic neurotransmission, among other biomarkers, before the onset of cognitive symptoms [6–11]. Evidence also supports that these abnormalities belong to a larger pathological framework that drives disease progression and cognitive decline [12–14]. As such, present research efforts focus on earlier intervention strategies to ameliorate AD pathology. Therapeutic targeting of pathogenesis before the onset of amyloid and tau proteinopathies and significant cognitive symptoms may prove more efficacious in attenuating disease symptomology.

Riluzole is a glutamatergic modulator currently FDA-approved for the treatment of amyotrophic lateral sclerosis (ALS). ALS treatment with riluzole has been shown to decrease presynaptic excitation and glutamate release through modulation of Na<sup>+</sup> and Ca<sup>2+</sup> channels [15–22] and support glutamatergic homeostasis through increased glutamate transporter expression and activity [23–27]. Previous studies also support the restoration of glutamatergic tone *in vivo* and improved spatial learning and memory performance in several AD mouse models [26, 28–31]. Our laboratory expanded on these findings by exploring prodromal riluzole treatment in a transgenic mouse model of AD (A $\beta$ PP/PS1). Similarly,

riluzole improved glutamatergic tone, spatial learning, and memory at 6 months post-treatment [32]. However, prior work does not address differences in on- and off-treatment effects, metabolic dysregulation, and sex differences in pathology and response to riluzole treatment.

Previous metabolic studies illustrate a relationship between hippocampal glutamate dynamics and glucose homeostasis. Impaired peripheral insulin tolerance resulting from high-fat diet insult elevates basal glutamate levels and stimulus-evoked glutamate release in the hippocampus of C57BL/6 male mice [12]. Findings from growth hormone receptor knock out longevity mouse models with increased insulin sensitivity indicate an opposing hypoglutamatergic environment in the hippocampus and enhanced cognition compared to littermate controls [33]. These results petition for further investigation into the modulation of glutamate dynamics as a strategy for combating metabolic dysfunction previously observed in transgenic male AD mice [12, 34, 35]. Riluzole recently underwent a Phase II clinical trial to treat mild AD (Clinical Trial #NCT01703117) in combination with donepezil, an acetylcholinesterase inhibitor. Patients receiving riluzole treatment for six months exhibited better cerebral glucose metabolism in several brain regions, including the posterior cingulate, hippocampus, and cortex [36]. Further, preservation of brain glucose metabolism was positively correlated with cognitive outcome measures at baseline and after riluzole treatment. Study outcomes are in agreement with previous research indicating increased glucose uptake rate and metabolism in the brain with riluzole treatment and support a possible connection between glutamatergic modulation by riluzole and glucose homeostasis on improving cognition in AD [37, 38].

This study seeks to provide insight into the efficacy of riluzole treatment on metabolic dysfunction and cognitive decline in both sexes of two amyloidogenic mouse models. The inclusion of female mice is imperative as prior research supports sex differences in metabolism [39, 40] and AD pathology [3, 41], possibly impacting responsiveness to riluzole intervention and subsequent metabolic and cognitive outcome measures. Further, the addition of an amyloidogenic knock-in mouse model of AD (APP<sup>NL-F/NL-F</sup>) will aid in avoiding confounding variables associated with transgenic mice, such as overexpression of the amyloid precursor protein and presenilin-1 [42]. We build on prior knowledge by including 6-month and 12-month time points to

determine on- and off-treatment effects on Morris water maze (MWM) performance and metabolic dysfunction in A $\beta$ PP/PS1 and APP<sup>NL-F/NL-F</sup> mice. Hippocampal plaque deposition begins at around 6 months old for both mouse models, with cognitive deficits observed at around 12 months of age [8, 35, 42, 43]. Our study targets an early intervention window (2–6 months of age) for these AD mouse models, with hippocampal glutamatergic dysregulation previously reported in A $\beta$ PP/PS1 male mice at this time point [7]. These efforts aim to investigate the efficacy of early glutamatergic modulation on metabolic regulation and cognition in AD pathology.

## MATERIALS AND METHODS

### Mice

Parental strains of C57BL/6 (RRID:IMSR JAX:000,664) and A $\beta$ PP/PS1 (RRID:MMRRC.034832-JAX) were obtained from Jackson Laboratory (Bar Harbor, ME), while APP<sup>NL-F/NL-F</sup> (RRID:IMSR\_RBRC06343) mice were obtained from Riken (Japan). Female breeders were paired with a male mouse and checked for pregnancy twice weekly, beginning 2 weeks after pairing. A $\beta$ PP/PS1 mice were paired with C57BL/6 mice, while APP<sup>NL-F/NL-F</sup> pairings included both heterozygous and homozygous mice for the APP<sup>NL-F/NL-F</sup> knock-in and C57BL/6 mice. Female C57BL/6 mice included in A $\beta$ PP/PS1 pairings were also used to backcross APP<sup>NL-F/NL-F</sup> mice. When selecting pairings, brother and sister mating was avoided. Pregnant female breeders were then separated from the male mouse and moved to a new cage with nesting material. New litters were tattooed with a corresponding mouse number and tail snipped for genotyping (TransnetYX) at 10 days old. Pups were weaned at approximately 23–28 days old and placed into sex-matched group housing of up to 5 mice total per cage from different litters to avoid interlitter variability.

Protocols for animal use were approved by the Institutional Animal Care and Use Committee at Southern Illinois University School of Medicine (Protocol #2022-055), which is accredited by the Association for Assessment and Accreditation of Laboratory Animal Care. Mice were group housed on a 12:12 h light-dark cycle, and food (Chow 5001 with 23.4% protein, 5% fat, and 5.8% crude fiber; LabDiet PMI Feeds) and water were available ad

libitum. All experiments were conducted during the light phase. Genotypes were confirmed by collecting a 5 mm tail snip for analysis by TransnetYX, Inc (Cordova, TN). The survival rate after weaning to the cessation of treatment and 6 months post-treatment remained consistent (>80%) in both the 6- and 12-month-old cohorts for APP<sup>NL-F/NL-F</sup> and C57BL/6 mice regardless of sex and treatment group, while A $\beta$ PP/PS1 male (50–70%) and female mice (23–65%) displayed a lower survival rate independent of treatment group.

### Riluzole treatment

The riluzole treatment paradigm timeline has been previously described [32]. All mice from three genotypes (C57BL/6, A $\beta$ PP/PS1, and APP<sup>NL-F/NL-F</sup>) and both sexes were randomly assigned by cage to receive either vehicle (1% sucrose) or riluzole treatment (12.5 mg/kg body weight (b.w.)/day) in their drinking water (*ad libitum*) from 2 to 6 months of age. A 1.78 mM stock solution of riluzole was made in deionized H<sub>2</sub>O with 1% sucrose and stored at –20°C. Every week, new water bottles were made by diluting aliquoted stock riluzole in 1% sucrose to a working concentration of 356  $\mu$ M, and mouse weights were recorded to determine treatment tolerance. Control mice received vehicle-treated drinking water and underwent the same weekly procedures as riluzole-treated mice.

### Intraperitoneal (IP) insulin and glucose tolerance testing (ITT/GTT)

After the cessation of riluzole treatment, mice in the 6-month group underwent an ITT, followed by a GTT approximately one week later, as previously described [12]. Mice in the 12-month group were off treatment for 6 months prior to ITT and GTT measures at approximately 12 months of age. For ITT, mice were fasted for 4 h before initial blood glucose measurements (time = 0) were taken from the tail vein using a Presto glucometer (AgaMatrix, Salem, NH, USA). Then, an IP injection of 1 IU/kg b.w. of insulin (Sanofi, France) was administered. For GTT, mice were fasted for 15 h before initial blood glucose measurements, and then an IP injection of 2 g of glucose/kg/b.w. was administered. After injection, blood glucose measurements were taken at 15, 30, 45, 60, and 120 min for both ITT and GTT.

## MWM

A week after ITT and GTT protocols were completed, we conducted an MWM assessment on all mice as previously described [7, 32, 44, 45]. Briefly, MWM examines spatial learning and long-term memory through requiring mice to utilize external visual cues to locate a hidden platform (submerged 1 cm below the opaque water surface), regardless of starting position in the pool. The MWM consists of one acclimation day, five consecutive learning days, and a probe challenge approximately 72 h following the last trial. The five learning days include three trials, up to 90 s in duration, starting from three different entry points into the pool (order is randomized throughout the learning days) with at least a 20-min inter-trial interval to test spatial learning capabilities. The probe challenge consists of a single 60-s trial with the platform removed from the pool to test long-term spatial memory. The ANY-maze video tracking system (Stoelting, Wood Dale, IL) tracks and analyzes several parameters, including average speed, cumulative distance from the platform, path efficiency to first platform entry, number of entries to the platform area, and time spent in each quadrant of the pool.

## Enzyme-linked immunosorbent assay (ELISA)

Blood samples were collected through cardiac puncture immediately following overdose with isoflurane, placed into an EDTA microvette tube, and spun at 1500 G for 10 min at 4°C. The separated plasma was stored in a -80°C freezer until further use. Blood chemistry analysis of circulating insulin and adiponectin concentration was carried out using Ultra-Sensitive Mouse ELISA kits (Crystal Chem, IL; Fujifilm, Japan) per the manufacturer's instructions. The Human/Rat  $\beta$  Amyloid (42) ELISA Kit (Fujifilm, Wako) was utilized to determine hippocampal soluble A $\beta$ <sub>42</sub> concentrations (experimental samples diluted 1:50). Hippocampal tissue was homogenized in 50 mM Tris Buffer (pH = 7.6) with protease inhibitor and centrifuged for 20 min at 4°C. Homogenates were aliquoted and stored at -80°C until quantification.

## Real-time polymerase chain reaction (RT-PCR)

Mice were euthanized with an overdose of isoflurane followed by rapid decapitation. Liver and hippocampal tissue were dissected (hippocampus on ice), tissue weight recorded, and then immedi-

ately stored at -80°C until RNA extraction. mRNA from hippocampal samples were extracted according to miRNeasy Mini Kit instructions (Qiagen). Liver mRNA was extracted by homogenization in Trizol Reagent and centrifugation at 12000 G for 15 min at 4°C with chloroform. RNA isolation was conducted using 100% isopropanol and identical centrifugation as before. Then, samples were washed with 75% EtOH and centrifugation at 7500 G for 5 min. Total RNA concentration was confirmed with NanoDrop One (Thermo Scientific). cDNA was synthesized with BioRad iScript cDNA synthesis kit following manufacturer instructions. For RT-PCR, individual samples were assayed with each reaction containing 10  $\mu$ L of iQ SYBR Green Supermix (BioRad, Hercules, CA, USA), 1  $\mu$ L each of forward and reverse primers, and 2.5  $\mu$ L diluted cDNA (3 H<sub>2</sub>O: 1 cDNA). Beta-2-microglobulin and ubiquitin-conjugating enzyme were used as controls for the liver and hippocampus, respectively, following previous studies from our laboratory [12]. Samples were run in duplicate, and results were averaged for data analysis. Forward and reverse primers are shown in Supplementary Table 1.

## Glycogen assay kit

Liver glycogen content was examined using a Glycogen Assay kit (Sigma-Aldrich) per the manufacturer's instructions. Liver tissue (10 mg) was homogenized in 100 mL of water on ice, boiled for 5 min for enzyme inactivation, and centrifuged for 5 min at room temperature. Homogenates were stored at -20°C until quantification.

## Statistical analysis

GraphPad Prism 9 Software (La Jolla, CA; RRID:SCR 002798) was used for statistical analyses. Statistical tests are listed in each figure legend. A single Grubb's test (alpha = 0.05) was utilized to identify significant outliers in each group. Exclusion criteria included seizure, injection failure (ITT/GTT), failure to learn (MWM), or death before the study ended. Failure to learn during the MWM was determined by comparing the cumulative distance from the platform on trial day 1 to the other 4 trial days and removing subjects that displayed the same or higher cumulative distance throughout the trial days. From the pool of mice included in ITT/GTT and MWM, a subset of mice from each treatment group and sex were chosen at random for RT-PCR and ELISA analysis. All

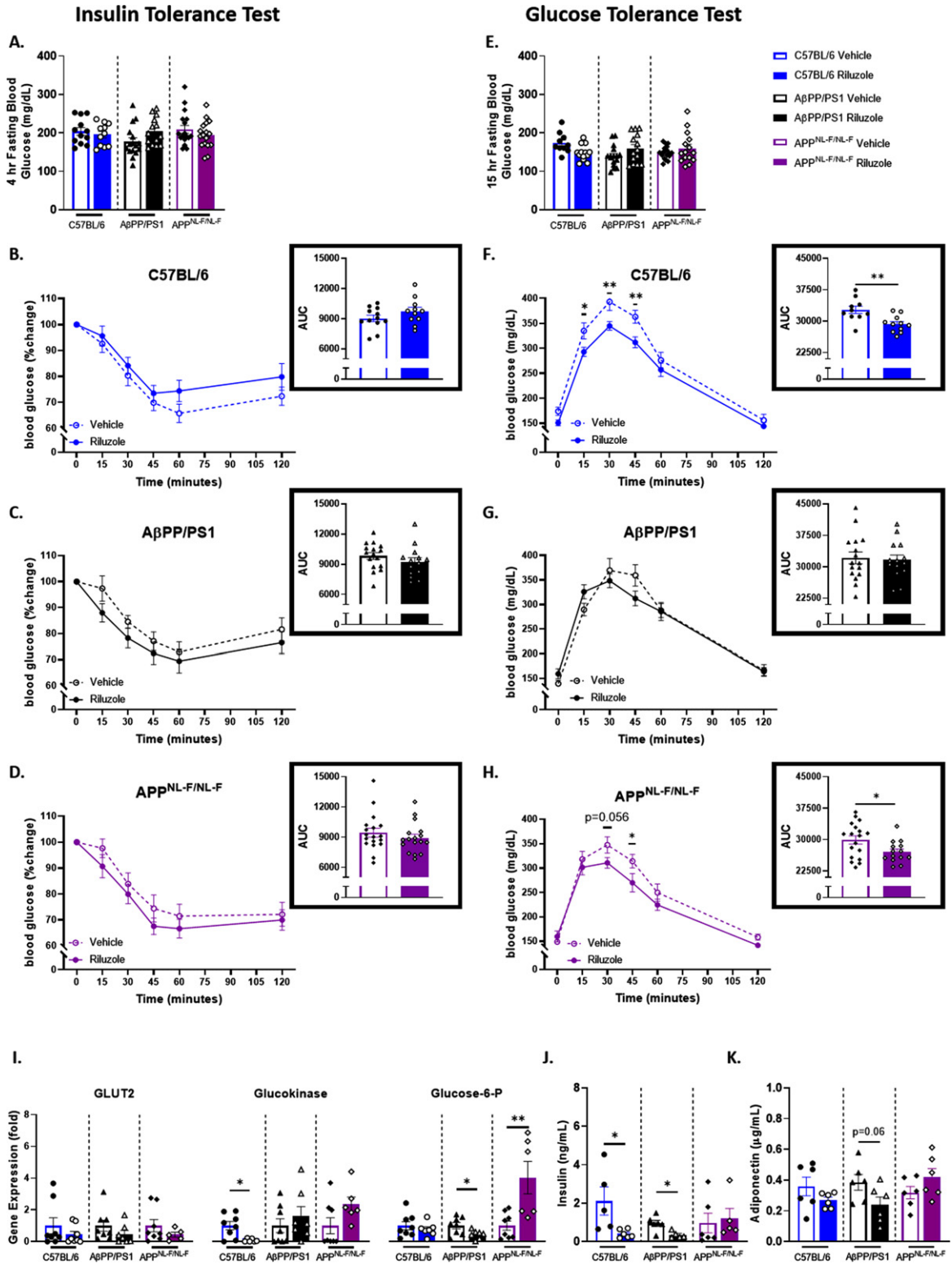


Fig. 1. (Continued)

mice included in the ELISA assay were also included in all measures of gene expression for RT-PCR. Data are represented as mean  $\pm$  SEM and statistical significance were defined as  $p < 0.05$ .

## RESULTS

### *Body weight changes*

All mice underwent voluntary oral administration of riluzole in their drinking water from 2–6 months of age. Daily consumption of riluzole was comparable to that of vehicle-treated mice (data not shown). Mouse weight was measured prior to treatment initiation and monitored weekly throughout the 4 months of riluzole administration. At 6 months old, male mice did not exhibit treatment effects for A $\beta$ PP/PS1, APP<sup>NL-F/NL-F</sup>, or C57BL/6 mice (Supplementary Figure 1A). Females at 6 months old showed significant treatment effects in weight gain for APP<sup>NL-F/NL-F</sup> mice ( $t(35) = 2.287$ ,  $p = 0.0283$ ) with riluzole-treated females gaining more weight than their genotype-matched vehicle-treated counterparts (Supplementary Figure 1B). No significant treatment effects were observed for A $\beta$ PP/PS1 or C57BL/6 female mice. Analysis of treatment-matched sex differences at 6 months of age revealed a significant main effect for A $\beta$ PP/PS1 mice ( $F(3,66) = 4.460$ ,  $p = 0.0065$ ), such that riluzole-treated A $\beta$ PP/PS1 male mice gained significantly more weight than A $\beta$ PP/PS1 female mice during treatment ( $p = 0.0121$ ). No sex differences were observed in vehicle-treated A $\beta$ PP/PS1 mice or either treatment group for APP<sup>NL-F/NL-F</sup> and C57BL/6 mice.

At 12 months old, riluzole-treated C57BL/6 male mice gained less weight than vehicle-treated genotype-matched male mice ( $t(27) = 2.600$ ,  $p = 0.0149$ ), while no differences were observed for A $\beta$ PP/PS1 and APP<sup>NL-F/NL-F</sup> male mice (Supplementary Figure 1C). Female A $\beta$ PP/PS1 mice displayed increased weight gain with riluzole treatment ( $t(25) = 2.267$ ,  $p = 0.0323$ ), but no significant

differences were observed for APP<sup>NL-F/NL-F</sup> or C57BL/6 mice (Supplementary Figure 1D). No significant sex differences were observed across all genotypes and treatment groups at this time point.

### *Alterations to peripheral glucose tolerance and homeostasis with riluzole treatment in male mice*

To discern the on-treatment effects of prodromal riluzole treatment on peripheral glucose tolerance and insulin sensitivity, we conducted ITT/GTT immediately following cessation of riluzole treatment at 6 months of age. No significant differences were observed for fasting glucose levels or insulin sensitivity after a 4-h fast in male mice (Fig. 1A–D). Fasting glucose levels also remained not significantly different after a 15-hour fast (Fig. 1E). However, GTT results support a significant main effect for treatment in APP<sup>NL-F/NL-F</sup> male mice ( $F(1,30) = 4.804$ ,  $p = 0.0363$ ) and C57BL/6 male mice ( $F(1,19) = 17.86$ ,  $p = 0.0005$ ) (Fig. 1E–H). Area under the curve (AUC) analysis also indicated significantly improved peripheral glucose tolerance with riluzole treatment for APP<sup>NL-F/NL-F</sup> ( $t(30) = 2.245$ ,  $p = 0.0323$ ) and C57BL/6 male mice ( $t(19) = 3.268$ ,  $p = 0.0041$ ), but not A $\beta$ PP/PS1 male mice. These findings indicated improved glucose tolerance in riluzole-treated APP<sup>NL-F/NL-F</sup> and C57BL/6 male mice, which may impact cognitive performance as previously described [12–14, 34].

To further investigate the observed improvement in peripheral glucose tolerance with riluzole treatment in the 6-month-old cohort, we conducted an RT-PCR analysis of liver tissue (Fig. 1I). Glucose transporter 2 (GLUT2) expression, a glucose transporter that facilitates glucose movement across the liver membrane, displayed no significant treatment effects in A $\beta$ PP/PS1, APP<sup>NL-F/NL-F</sup>, or C57BL/6 male mice. Examination of glucokinase, an enzyme that facilitates the phosphorylation of glucose to glucose-6-phosphate, supported decreased expression with riluzole treatment in C57BL/6 male mice alone ( $t(12) = 2.962$ ,  $p = 0.0119$ ). Glucose-6-phosphatase

Fig. 1. Riluzole improves peripheral glucose tolerance in male APP<sup>NL-F/NL-F</sup> mice and littermate C57BL/6 mice at 6 months of age. A) Blood glucose levels acquired from the tail vein after a 4 hour fast. B–D) Insulin tolerance was measured by percent change from baseline ( $T=0$ ). Insets depict percent change AUC for each genotype (C57BL/6, A $\beta$ PP/PS1, and APP<sup>NL-F/NL-F</sup>) and treatment group. E) Blood glucose levels obtained from the tail vein after a 15-h fast. F–H) Blood glucose levels measured on the same time course as previously described following IP injection of glucose. Insets show AUC for each genotype and treatment group. I) RT-PCR analysis of liver tissue. J, K) ELISA quantification of serum insulin and adiponectin levels. ITT/GTT time course, within-genotype repeated measures two-way ANOVA, Fisher's LSD; AUC ( $n = 10$ –18), RT-PCR ( $n = 6$ –8), and ELISA analysis ( $n = 5$ –6) within-genotype unpaired  $t$ -test, \* $p < 0.05$ , \*\* $p < 0.01$ .

(G6P), an enzyme responsible for hydrolyzing glucose-6-phosphate, indicated increased expression of G6P in riluzole-treated male APP<sup>NL-F/NL-F</sup> mice ( $t(12)=3.243$ ,  $p=0.0070$ ). A $\beta$ PP/PS1 male mice showed a significant opposing result with a decrease in G6P expression with riluzole treatment ( $t(13)=2.399$ ,  $p=0.0313$ ).

Additionally, circulating insulin and adiponectin levels were examined for each genotype and treatment group to provide context for possible changes to glucose regulation. ELISA quantification of serum insulin concentration revealed a significant decrease with riluzole treatment for male A $\beta$ PP/PS1 mice ( $t(9)=3.219$ ,  $p=0.0105$ ) and C57BL/6 mice ( $t(9)=2.553$ ,  $p=0.0310$ ), while no differences were observed for APP<sup>NL-F/NL-F</sup> male mice (Fig. 1J). A decrease in serum adiponectin levels was also observed for riluzole-treated A $\beta$ PP/PS1 male mice alone (Fig. 1K). To further examine possible impacts on glucose storage, we conducted a glycogen assay in liver tissue. No significant differences were observed across all genotypes (Supplementary Figure 2). Together, these findings may indicate genotype-specific alterations to glucose homeostasis with riluzole treatment.

#### *Improved spatial cognitive performance in C57BL/6 male mice with riluzole treatment*

Further, we conducted a hidden-platform MWM task to investigate the on-treatment effects of riluzole on learning and spatial memory. No significant differences were observed for male mice in spatial learning ability, and all mice were able to learn the location of the platform by trial day five (Fig. 2A-C). Probe challenge results indicated no significant treatment difference in long-term spatial memory performance for either APP<sup>NL-F/NL-F</sup> or A $\beta$ PP/PS1 male mice at 6 months of age (Fig. 2D-F). No significant differences were observed for swim speed during the learning trials and probe challenge for any mice (data not shown). However, riluzole-treated C57BL/6 male mice did exhibit a significant increase in platform entries during the probe challenge ( $t(18)=2.758$ ,  $p=0.0130$ ) (Fig. 2D) and displayed significant selective searching behavior in both the vehicle-treated ( $F(3,36)=23.60$ ,  $p<0.0001$ ) and riluzole-treated groups ( $F(3,36)=23.08$ ,  $p<0.0001$ ) (Fig. 2F). Significant selective searching was also observed for APP<sup>NL-F/NL-F</sup> mice regardless of treatment (vehicle:  $F(3,48)=12.73$ ,  $p<0.0001$ ); riluzole:  $F(3,52)=14.95$ ,  $p<0.0001$ ), but was absent for

vehicle-treated A $\beta$ PP/PS1 mice. An improvement in preference for the target quadrant compared to the other quadrants of the pool was observed with riluzole treatment for A $\beta$ PP/PS1 male mice ( $F(3,48)=23.24$ ,  $p<0.001$ ). Path traces from the probe challenge illustrate these genotype-specific search strategies (Fig. 2G).

ELISA quantification of soluble A $\beta_{42}$  in the hippocampus revealed no significant effect of riluzole treatment on A $\beta_{42}$  levels in 6-month-old AD mice (Fig. 2H). To probe central targets in glutamatergic neurotransmission and glucose homeostasis, we performed RT-PCR analysis on hippocampal tissue. GluN2A, a predominately synaptic N-methyl-D-aspartate receptor (NMDAR2A) subtype, was selected to characterize NMDAR expression and for its role in long-term potentiation and learning and memory [46]. NMDAR2A expression has also been shown to be significantly impacted by prodromal riluzole treatment in 6-month-old transgenic (5XFAD) male mice utilizing the same treatment protocol [30]. Yet, NMDAR2A showed no significant treatment effects across all genotypes (Fig. 2I).  $\alpha 7$  nicotinic acetylcholine receptor ( $\alpha 7$ nAChR) expression was also investigated as it has previously been shown to elicit presynaptic glutamate release, including through high-affinity binding by A $\beta_{42}$  [47, 48], and form a complex with NMDAR2A at the postsynaptic membrane impacting memory performance [49, 50]. C57BL/6 male mice exhibited significantly reduced  $\alpha 7$  nicotinic acetylcholine receptor ( $\alpha 7$ nAChR) expression with riluzole treatment ( $t(14)=2.580$ ,  $p=0.0218$ ) (Fig. 2J). No significant treatment effects were observed for A $\beta$ PP/PS1 or APP<sup>NL-F/NL-F</sup> male mice. Glucose transporters 1 and 3 (GLUT1, GLUT3) were examined to characterize glucose uptake in neurons (GLUT3), alongside uptake into glial cells and across the blood-brain barrier (GLUT1) into the brain (Fig. 2K). A $\beta$ PP/PS1 male mice showed a significant reduction in GLUT1 with riluzole treatment ( $t(13)=3.523$ ,  $p=0.0037$ ), while no significant differences were observed for APP<sup>NL-F/NL-F</sup> or C57BL/6 mice. GLUT3 results demonstrated opposing differences between genotypes as riluzole-treated C57BL/6 male mice exhibited significantly increased expression ( $t(12)=2.771$ ,  $p=0.0169$ ) and A $\beta$ PP/PS1 a decrease ( $t(13)=2.165$ ,  $p=0.0496$ ). The insulin receptor (INSR) and adiponectin R1 receptor (AdipoR1) were examined as primary modulators of glucose homeostasis alongside their downstream target cyclic AMP (cAMP) response element-binding protein 1

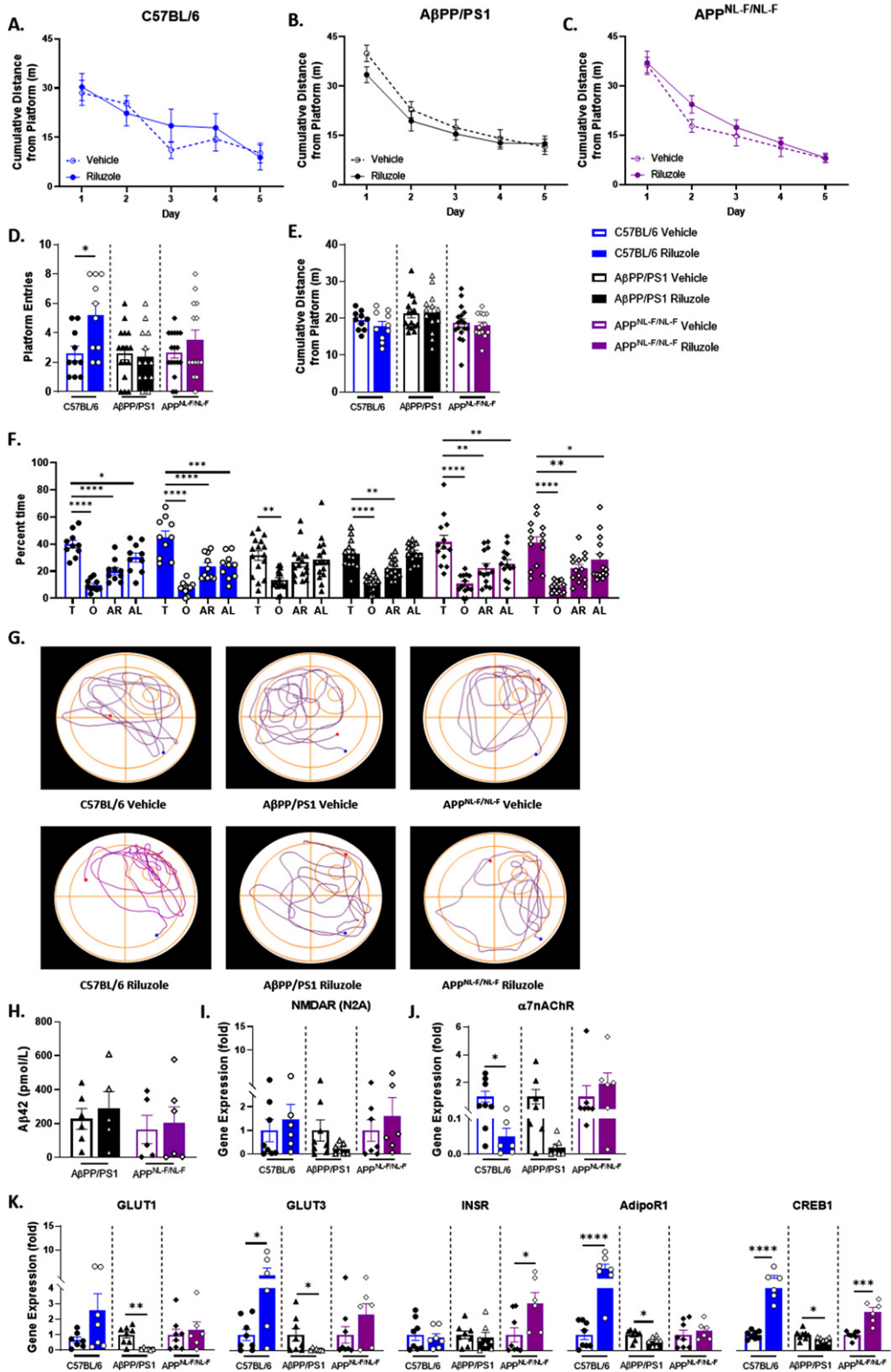


Fig. 2. (Continued)

(CREB1) (Fig. 2K). Riluzole-treated APP<sup>NL-F/NL-F</sup> male mice alone had significantly increased INSR expression ( $t(12)=2.541, p=0.0259$ ). AdipoR1 and CREB1 showed opposing results between genotypes, as C57BL/6 male mice saw a significant increase in expression ( $t(14)=5.999, p<0.0001$ ;  $t(13)=7.034, p<0.0001$ ) and A $\beta$ PP/PS1 mice a decrease ( $t(13)=2.464, p=0.0284$ ;  $t(13)=2.339, p=0.0360$ ) with riluzole treatment. APP<sup>NL-F/NL-F</sup> male mice exhibited a significant increase in CREB1 expression with riluzole treatment ( $t(12)=5.581, p=0.0001$ ). Together, these findings indicate possible on-treatment procognitive effects for male C57BL/6 mice and changes to glucose transport and insulin and adiponectin signaling pathways with riluzole treatment for all genotypes.

#### *Enhanced insulin sensitivity with riluzole treatment in female C57BL/6 mice*

To elucidate possible sex-dependent effects on peripheral glucose homeostasis and spatial cognition, the same ITT/GTT and MWM protocol was carried out in female mice at 6 months of age. ITT results supported no main effect in the glucose monitoring time course across all genotypes (Fig. 3A-D). However, when taken together, AUC analysis indicated a significant improvement in insulin sensitivity for riluzole-treated compared to vehicle-treated C57BL/6 female mice ( $t(20)=2.094, p=0.0492$ ) (Fig. 3B). GTT results indicate no significant treatment effects for APP<sup>NL-F/NL-F</sup>, A $\beta$ PP/PS1, and C57BL/6 mice for fasting glucose levels and glucose tolerance (Fig. 3E-H). RT-PCR analysis of liver tissue revealed no significant treatment effects across all genotypes for GLUT2 and glucokinase (Fig. 3I). APP<sup>NL-F/NL-F</sup> mice showed significantly lower G6P expression with riluzole treatment ( $t(13)=2.807, p=0.0148$ ), while no differences were observed for A $\beta$ PP/PS1 or C57BL/6 mice. ELISA quantification of serum insulin and adiponectin levels (Fig. 3J-K) and examination of liver glycogen also indicated no significant treatment effects across all genotypes (Supplementary Figure 2). These findings

indicate modest improvement in insulin sensitivity for riluzole-treated C57BL/6 female mice alone, supporting sex differences in glucose homeostasis and response to riluzole treatment for APP<sup>NL-F/NL-F</sup> and C57BL/6 mice.

#### *Spatial learning performance improved with riluzole treatment in A $\beta$ PP/PS1 female mice*

For MWM, no treatment effects were observed for spatial learning for APP<sup>NL-F/NL-F</sup> or C57BL/6 female mice (Fig. 4A-C). Examination of AUC for the five trial days showed improved spatial learning for A $\beta$ PP/PS1 riluzole-treated female mice compared to genotype-matched vehicle-treated mice ( $t(19)=2.016, p=0.0582$ ) (Fig. 4B). Probe challenge swimming speed (data not shown) was nonsignificant across all genotypes and treatment groups. All vehicle-treated female mice showed no preference for the target quadrant compared to the other three quadrants, which was improved with riluzole treatment for all genotypes [(C57:  $F(3,40)=15.73, p<0.001$ ); (PS1:  $F(3,40)=7.959, p=0.0003$ ); (NLF:  $F(3,32)=11.51, p<0.0001$ )] (Fig. 4D-F). Representative probe challenge paths are shown in Fig. 4G.

ELISA quantification of soluble A $\beta_{42}$  indicated no significant treatment effects on A $\beta_{42}$  levels in the hippocampus for female AD mice (Fig. 4H). APP<sup>NL-F/NL-F</sup> female mice alone displayed decreased NMDAR2A expression with riluzole treatment (Fig. 4I). Riluzole-treated C57BL/6 female mice alone exhibited significantly decreased  $\alpha 7$ nAChR expression ( $t(12)=2.187, p=0.0493$ ) (Fig. 4J). GLUT1 showed no treatment effects across all genotypes (Fig. 4K). Increased GLUT3 expression was observed in APP<sup>NL-F/NL-F</sup> female mice with riluzole treatment. No significant differences were observed for C57BL/6 or A $\beta$ PP/PS1 female mice (Fig. 4K). A $\beta$ PP/PS1 riluzole-treated females alone showed significantly increased INSR expression ( $t(13)=2.209, p=0.0457$ ). Female C57BL/6 mice alone saw significantly increased AdipoR1 ( $t(11)=7.800, p<0.0001$ ) and CREB1 ( $t(11)=2.905, p=0.0143$ ) expression with riluzole

Fig. 2. Selective on-treatment changes in spatial cognitive performance with riluzole treatment at 6 months old. A-C) Spatial learning performance measured by proximity to the platform throughout the trial days. D, E) Platform entries and cumulative distance from the platform during the probe challenge, respectively. F) Analysis of probe challenge quadrant occupancy (T: target, O: opposite, AR: adjacent right, AL: adjacent left) with percent time. G) Track plots of each genotype and treatment group during the probe challenge. H) ELISA quantification of soluble A $\beta_{42}$  levels in the hippocampus. I-K) RT-PCR analysis of gene targets in hippocampal tissue. Learning trials two-way repeated measures ANOVA, Sidak ( $n=10-17$ ); probe challenge, RT-PCR ( $n=6-8$ ), and ELISA analysis ( $n=5-6$ ) within-genotype unpaired  $t$ -test; Quadrant occupancy one-way ANOVA, Dunnett's, \* $p<0.05$ , \*\* $p<0.01$ , \*\*\* $p<0.001$ , \*\*\*\* $p<0.0001$ .

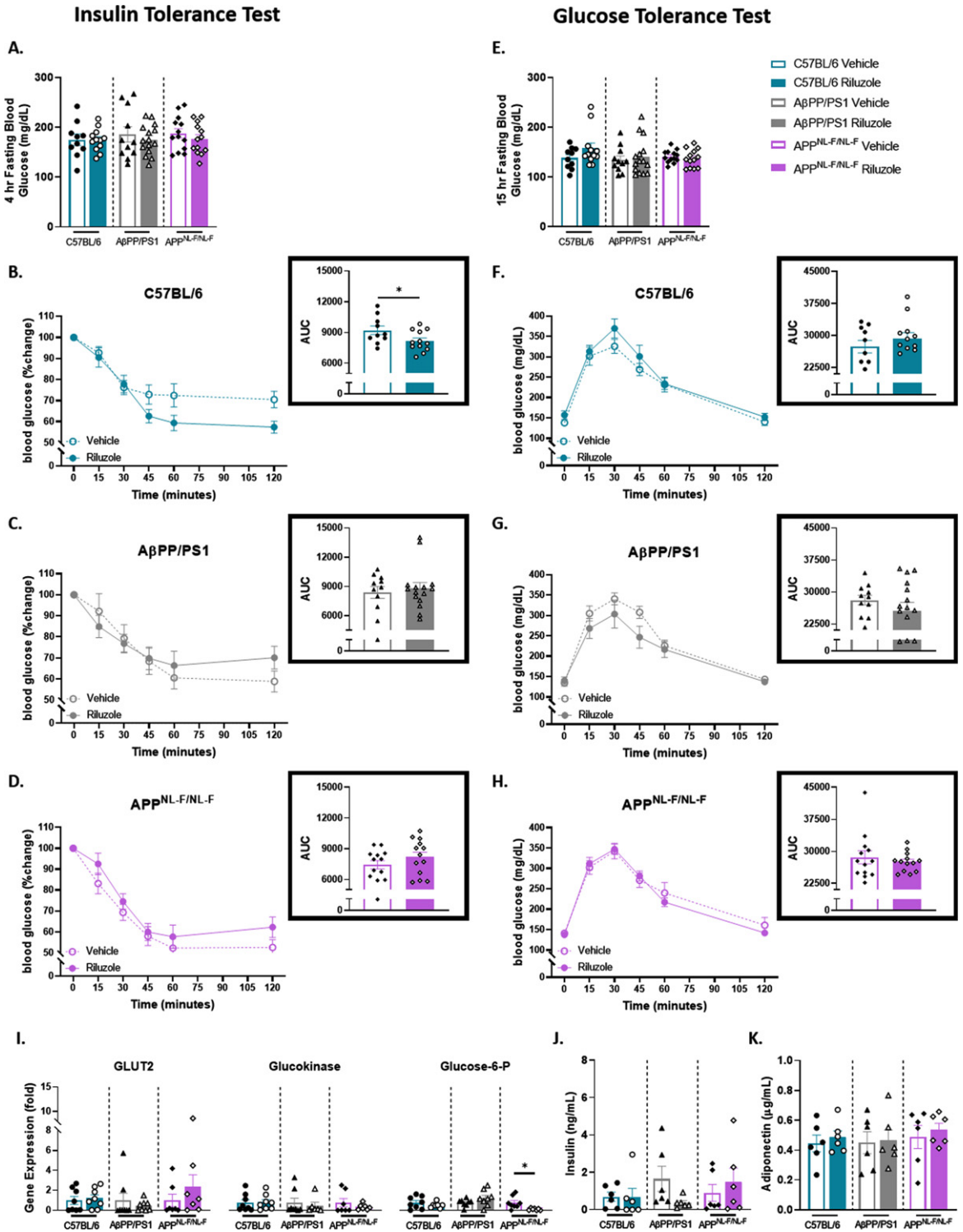


Fig. 3. (Continued)

treatment (Fig. 4K). Collectively, data support improved spatial learning performance in A $\beta$ PP/PS1 female mice with riluzole treatment that may work through the insulin signaling pathway to elicit the procognitive effects observed and improved spatial long-term memory performance across all genotypes for riluzole-treated female mice.

#### *Off-treatment alterations to key factors in glucose homeostasis in riluzole-treated mice*

To determine possible long-term effects of prodromal riluzole treatment, we conducted ITT/GTT and MWM analysis on a separate cohort of mice six months after treatment cessation. No significant treatment effects were observed for peripheral insulin or glucose tolerance in either sex at 12 months of age (Supplementary Figure 3). RT-PCR analysis of liver tissue from male mice indicated that 12-month-old APP<sup>NL-F/NL-F</sup> mice displayed significantly decreased GLUT2 expression with riluzole treatment ( $t(14)=2.505$ ,  $p=0.0252$ ) (Fig. 5A). No significant differences were observed for A $\beta$ PP/PS1 and C57BL/6 male mice. Significantly increased glucokinase expression was observed in A $\beta$ PP/PS1 male mice with riluzole treatment ( $t(11)=2.540$ ,  $p=0.0275$ ), while no significant differences were observed for APP<sup>NL-F/NL-F</sup> and C57BL/6 mice. Riluzole-treated A $\beta$ PP/PS1 male mice alone also showed increased G6P expression. Quantification of circulating insulin levels revealed that male A $\beta$ PP/PS1 mice alone continued to show significantly decreased insulin levels with riluzole treatment ( $t(9)=2.327$ ,  $p=0.0450$ ) (Fig. 5B). No significant differences were observed for adiponectin levels (Fig. 5C) or liver glycogen in male mice (Supplementary Figure 2). For female mice, decreased GLUT2 expression in riluzole-treated APP<sup>NL-F/NL-F</sup> mice was observed, with no treatment effects for A $\beta$ PP/PS1 or C57BL/6 mice (Fig. 5D). Female mice showed no treatment effects for glucokinase and G6P across all genotypes. Female mice showed no significant treatment effects in serum insulin and adiponectin concentration (Fig. 5E, F) or

liver glycogen (Supplementary Figure 2). Together, these findings indicate modest off-treatment effects on the expression of key glucose metabolism factors in both male and female mice that did not confer an effect on insulin and glucose tolerance testing.

#### *Procognitive effects with prodromal riluzole treatment in male AD mice*

MWM results supported no significant differences in spatial learning throughout the trial days for male mice, and all mice were able to locate the platform by trial day five (Fig. 6A-C). During the probe challenge, no significant differences were observed in average swim speed across all genotypes (data not shown). Male APP<sup>NL-F/NL-F</sup> mice showed a significantly increased number of platform entries ( $t(36)=2.453$ ,  $p=0.0192$ ) with riluzole treatment (Fig. 6D). No significant differences in platform entries were observed for A $\beta$ PP/PS1 or C57BL/6 male mice. However, riluzole-treated male A $\beta$ PP/PS1 mice stayed in significantly closer proximity to the platform area than vehicle-treated genotype-matched mice ( $t(30)=2.160$ ,  $p=0.0389$ ) (Fig. 6E). No significant differences in cumulative distance were observed for APP<sup>NL-F/NL-F</sup> or C57BL/6 mice. Vehicle-treated C57BL/6 male mice displayed significant selective searching behavior ( $F(3,56)=21.49$ ,  $p<0.0001$ ), while riluzole-treated C57BL/6 mice lacked selectivity (Fig. 6F). Selective searching was also significant in riluzole-treated male APP<sup>NL-F/NL-F</sup> mice ( $F(3,80)=16.06$ ,  $p<0.0001$ ) but not in vehicle-treated APP<sup>NL-F/NL-F</sup> mice. A $\beta$ PP/PS1 male mice failed to show selective searching in either treatment group. Representative swimming paths from the probe challenge appear to possibly illustrate a circling swim strategy in male A $\beta$ PP/PS1 mice, while APP<sup>NL-F/NL-F</sup> mice may show a more targeted direct swim and rotating swim strategy (Fig. 6G). This divergence in swim strategies between the AD models could impact the parameter by which improved long-term spatial memory was observed.

Fig. 3. Female AD mice fail to show improved glucose tolerance with riluzole treatment similar to littermate C57BL/6 mice at 6 months of age. A) Blood glucose levels acquired from the tail vein after a 4-h fast. B-D) Insulin tolerance was measured by percent change from baseline ( $T=0$ ). Insets show AUC for each genotype and treatment group. E) Blood glucose levels obtained from the tail vein after a 15-h fast. F-H) Two-hour monitoring of blood glucose levels following an IP injection of glucose. Insets displays AUC. I) RT-PCR analysis of liver tissue. J-K) ELISA quantification of serum insulin and adiponectin levels. ITT/GTT time course, within-genotype repeated measures two-way ANOVA, Fisher's LSD; AUC ( $n=10-15$ ), RT-PCR ( $n=6-8$ ), and ELISA analysis ( $n=5-6$ ), within-genotype unpaired  $t$ -test,  $*p<0.05$ ,  $**p<0.01$ .

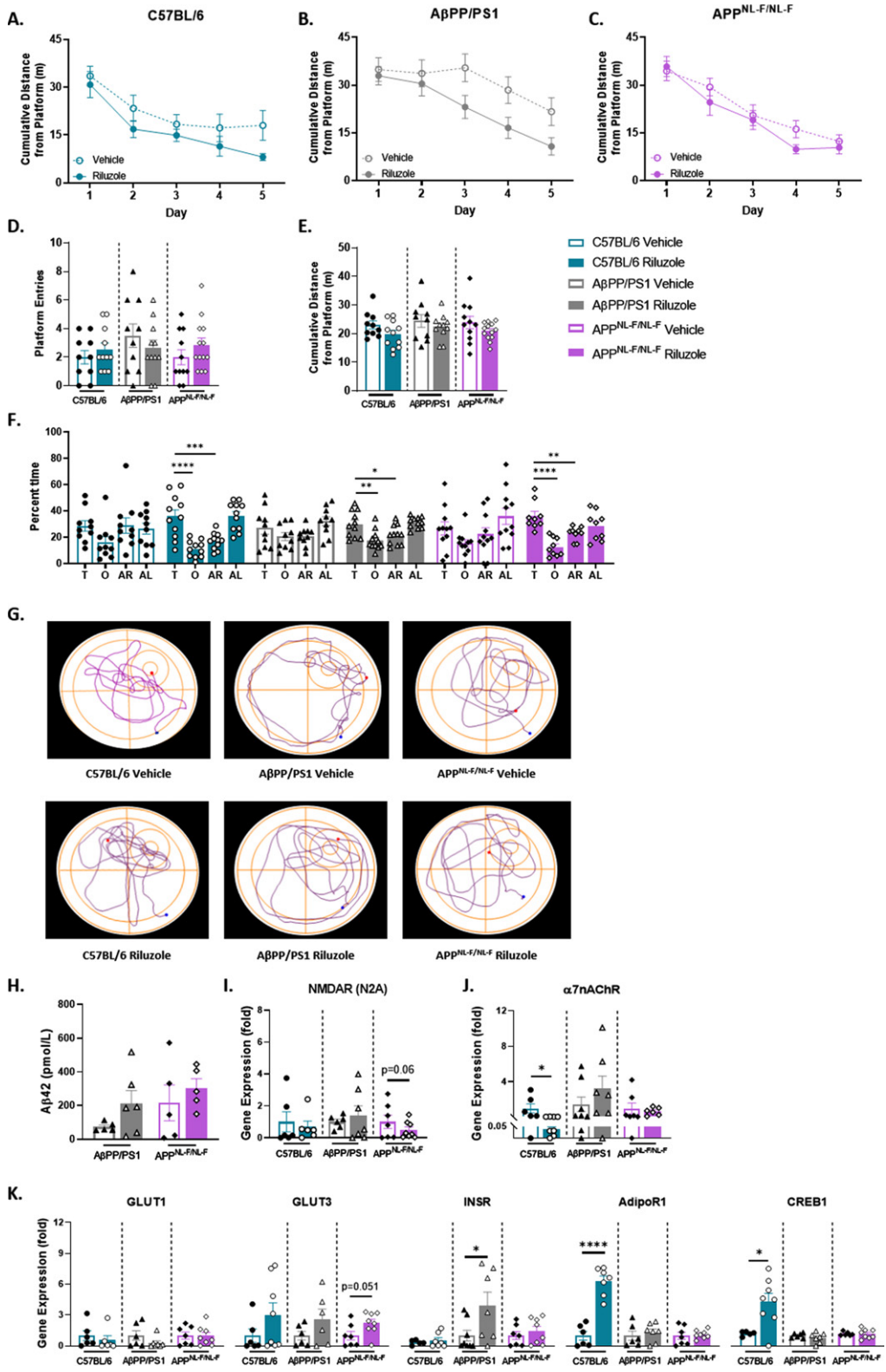


Fig. 4. (Continued)

Quantification of hippocampal soluble A $\beta$ <sub>42</sub> supported no significant differences in A $\beta$ <sub>42</sub> concentration with riluzole treatment for A $\beta$ PP/PS1 and APP<sup>NL-F/NL-F</sup> male mice (Fig. 6H). No significant differences were observed in NMDAR2A expression for any male mice (Fig. 6I). Control male mice continued to show significantly decreased  $\alpha$ 7nAChR expression with riluzole treatment ( $t(14)=2.580$ ,  $p=0.0218$ ) (Fig. 6J). A $\beta$ PP/PS1 riluzole-treated male mice also showed decreased  $\alpha$ 7nAChR expression, while APP<sup>NL-F/NL-F</sup> mice displayed increased expression with riluzole treatment.

Riluzole-treated C57BL/6 mice also had significantly decreased GLUT1 ( $t(13)=2.319$ ,  $p=0.0373$ ), GLUT3 ( $t(14)=3.154$ ,  $p=0.0070$ ), INSR ( $t(14)=3.344$ ,  $p=0.0048$ ), and CREB1 ( $t(14)=2.643$ ,  $p=0.0193$ ) expression (Fig. 6K). A decrease in AdipoR1 was also observed for C57BL/6 mice with riluzole treatment. A $\beta$ PP/PS1 male mice exhibited significantly decreased GLUT3 ( $t(12)=4.068$ ,  $p=0.0016$ ), INSR ( $t(12)=2.327$ ,  $p=0.0383$ ), and CREB1 ( $t(12)=3.001$ ,  $p=0.0110$ ) expression with riluzole treatment. Significantly increased expression of CREB1 ( $t(14)=2.287$ ,  $p=0.0383$ ) alone was observed for riluzole-treated APP<sup>NL-F/NL-F</sup> male mice. Together, these results support possible off-treatment effects for glucose transport, insulin signaling, and spatial cognition in AD male mice.

#### *Altered soluble hippocampal A $\beta$ <sub>42</sub> with riluzole treatment in female AD mice*

Results from the female cohort indicated no significant treatment effects in spatial learning, and all mice learned the platform location (Fig. 7A-C). No significant differences were observed for swim speed across all genotypes (data not shown). Female C57BL/6 mice alone exhibited significantly increased platform entries with riluzole treatment ( $t(28)=2.052$ ,  $p=0.0496$ ) (Fig. 7D). No differences were observed for cumulative distance across all genotypes (Fig. 7E). Selective searching behavior was observed in APP<sup>NL-F/NL-F</sup> female mice alone with riluzole treatment ( $F(3,64)=12.39$ ,  $p<0.0001$ )

(Fig. 7F). A nonselective swim pattern was observed with riluzole treatment in A $\beta$ PP/PS1 female mice, indicating a loss of any preference for the target quadrant that was present in vehicle-treated A $\beta$ PP/PS1 female mice ( $F(3,56)=10.22$ ,  $p<0.0001$ ). Decreased preference for the target quadrant with riluzole treatment was also observed for C57BL/6 female mice ( $F(3,56)=17.50$ ,  $p<0.0001$ ) compared to vehicle-treated C57BL/6 sex-matched mice ( $F(3,56)=12.38$ ,  $p<0.0001$ ). Path traces from the probe challenge indicate a similar swim strategy across all groups (Fig. 7G). Results from the MWM indicate selective and modest off-treatment effects on long-term spatial memory for C57BL/6 and APP<sup>NL-F/NL-F</sup> female mice.

ELISA quantification of soluble A $\beta$ <sub>42</sub> in the hippocampus revealed significantly increased A $\beta$ <sub>42</sub> concentration with riluzole treatment for female A $\beta$ PP/PS1 mice ( $t(8)=4.654$ ,  $p=0.0016$ ) (Fig. 7H). Riluzole-treated APP<sup>NL-F/NL-F</sup> female mice showed reduced A $\beta$ <sub>42</sub> concentration compared to genotype-matched vehicle-treated mice. C57BL/6 female mice alone exhibited decreased NMDAR2A expression with riluzole treatment (Fig. 7I). A $\beta$ PP/PS1 riluzole-treated female mice alone showed decreased  $\alpha$ 7nAChR expression (Fig. 7J). Further, A $\beta$ PP/PS1 female mice showed significantly decreased GLUT1 and GLUT3 expression with riluzole treatment ( $t(14)=3.977$ ,  $p=0.0014$ ;  $t(13)=3.595$ ,  $p=0.0033$ ), while riluzole-treated C57BL/6 females saw a significant increase in GLUT1 ( $t(14)=2.460$ ,  $p=0.0275$ ) (Fig. 7K). C57BL/6 female mice also showed increased GLUT3 and decreased INSR expression with riluzole treatment. No differences in glucose transport or INSR expression were observed for APP<sup>NL-F/NL-F</sup> female mice. However, female APP<sup>NL-F/NL-F</sup> mice did show significantly increased CREB1 expression with riluzole treatment ( $t(15)=2.358$ ,  $p=0.0324$ ) (Fig. 7K). Data support alterations to amyloid pathology and CREB expression for riluzole-treated APP<sup>NL-F/NL-F</sup> females that may contribute to improved long-term memory performance during the MWM task. Conversely, the significant rise in soluble A $\beta$ <sub>42</sub> observed in female A $\beta$ PP/PS1 mice

Fig. 4. Improved spatial learning performance in riluzole-treated A $\beta$ PP/PS1 female mice at 6 months old. A-C) Cumulative distance from the platform area throughout the spatial learning trials. Probe challenge measures include: platform entries (D), cumulative distance from platform (E), and quadrant occupancy (F). G) Track plots of each genotype and treatment group during the probe challenge. H) ELISA quantification of soluble A $\beta$ <sub>42</sub> levels in the hippocampus. I-K) RT-PCR analysis of gene targets in hippocampal tissue. Learning trials two-way repeated measures ANOVA, Sidak ( $n=10-13$ ); AUC learning trials, probe challenge, RT-PCR ( $n=6-8$ ), and ELISA analysis ( $n=5-6$ ) within-genotype unpaired  $t$ -test; Quadrant occupancy one-way ANOVA, Dunnett's (H), \* $p<0.05$ , \*\* $p<0.01$ , \*\*\* $p<0.001$ , \*\*\*\* $p<0.0001$ .

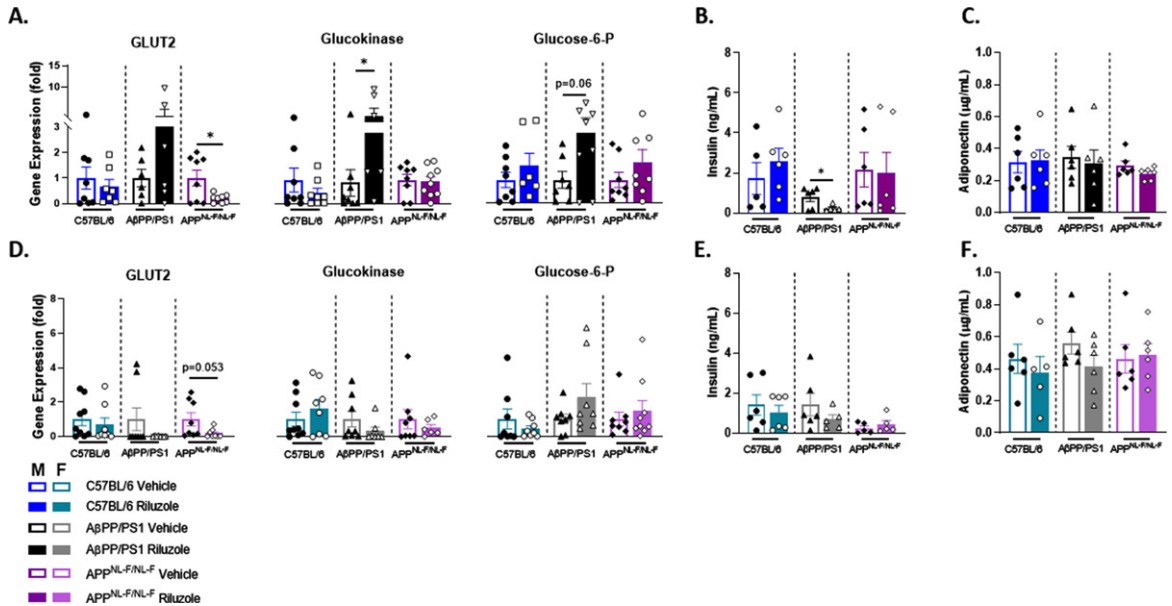


Fig. 5. Off-treatment sex-dependent changes to peripheral glucose homeostatic factors in riluzole-treated AD mice. A) RT-PCR analysis of liver tissue in 12-month-old male mice for each genotype and treatment group. B, C) ELISA quantification of serum insulin (B) and adiponectin (C) levels for male mice. D-F) RT-PCR analysis of liver tissue (D) and ELISA quantification of serum insulin (E) and adiponectin (F) levels in female mice for each genotype and treatment group. Within-genotype unpaired *t*-test, \* $p < 0.05$ , ( $n = 6-10$ ).

with riluzole treatment could possibly explain in part the loss of target quadrant preference. Taken together, these findings indicate off-treatment sex- and genotype-dependent effects of prodromal riluzole treatment on swim strategy, long-term memory, amyloid pathology, and glucose homeostasis in AD mice.

## DISCUSSION

This study aimed to investigate the on- and off-treatment effects of prodromal riluzole treatment on the modulation of glutamatergic receptors, glucose homeostasis, and cognition. To this end, separate cohorts of 6- and 12-month-old male and female A $\beta$ PP/PS1, APP<sup>NL-F/NL-F</sup>, and C57BL/6 mice received either riluzole- or vehicle-treated drinking water from 2-6 months of age. The cohorts were assayed either immediately following treatment cessation (6 months of age) or 6 months post-treatment (12 months of age). This intervention was implemented before the onset of cognitive decline for both AD mouse models and at a time point when hippocampal glutamatergic hyperactivity was previously observed in A $\beta$ PP/PS1 male mice [7]. These factors are thought to be interrelated with metabolic dysfunction in AD pathology and underlie cognitive

decline in later disease stages [51, 52]. Our findings indicated a sex- and genotype-specific response to prodromal riluzole intervention, highlighting the possibility of a specific optimal intervention window to maximize the observed benefits of glutamatergic modulation (Supplementary Table 2).

### *Altered metabolic tolerance in male AD mice with riluzole treatment*

Results from ITT and GTT experiments demonstrated improved peripheral glucose tolerance for riluzole-treated APP<sup>NL-F/NL-F</sup> and C57BL/6 male mice at 6 months old. No treatment-related metabolic differences were observed for A $\beta$ PP/PS1 mice. This contradicts previous studies that observed peripheral metabolic dysregulation in A $\beta$ PP/PS1 mice, potentially emerging as early as 2 months of age [53]. ITT/GTTs conducted at differing time points have yielded varying results between laboratories. One study reported impaired fasting glucose and insulin tolerance in 6-month-old A $\beta$ PP/PS1 mice, while no differences were seen at 3 months old [8]. Other studies have reported impaired glucose tolerance and increased plasma insulin at 2-4 months old [53, 54]. Peripheral metabolic deregulation is more commonly reported at later disease stages (>8 months old) [53, 55, 56]. However, other laboratories have reported

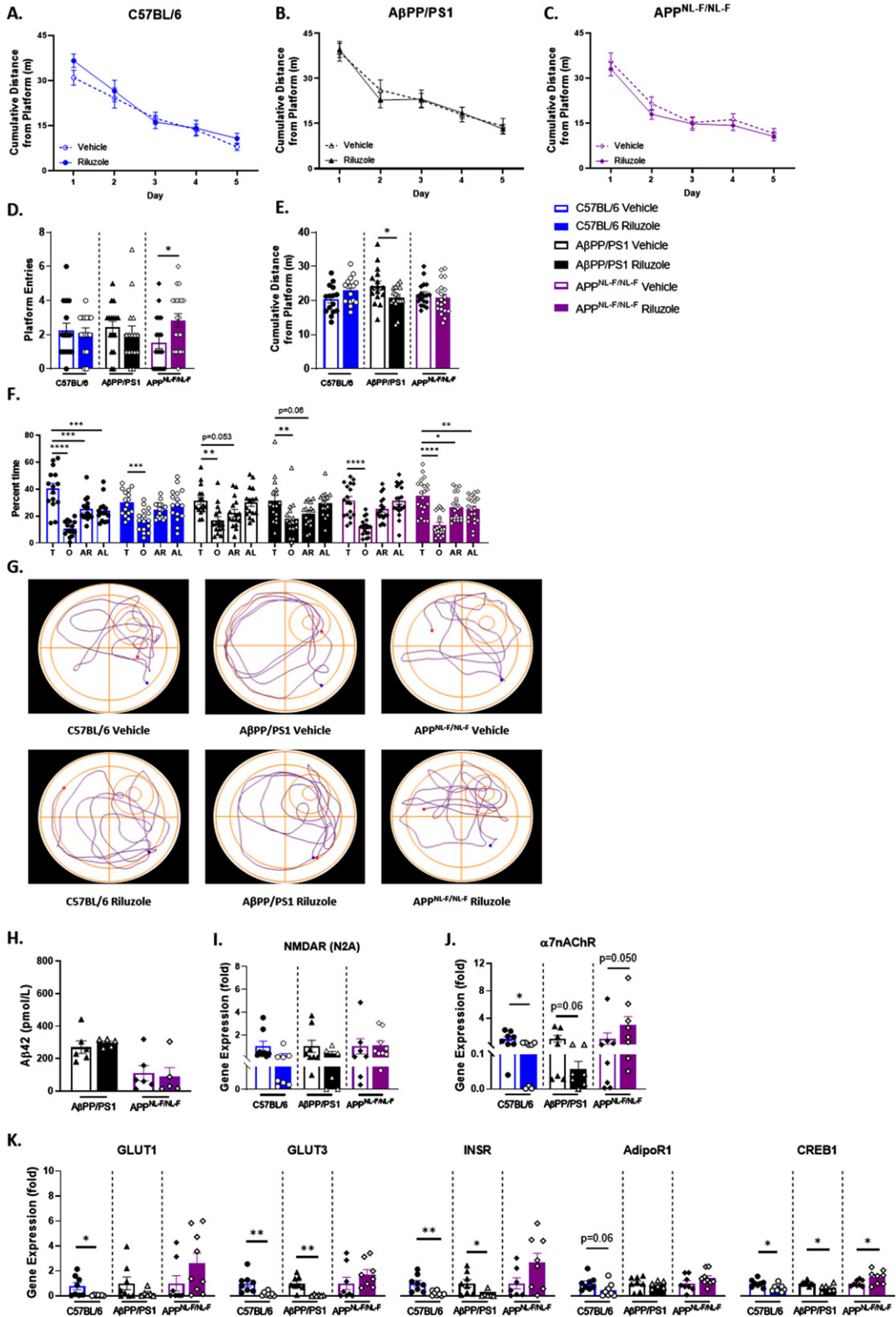


Fig. 6. (Continued)

normal glucose tolerance in A $\beta$ PP/PS1 mice at pre- and post-cognitive deficit onset time points [41, 57]. The lack of congruency between laboratories could result from a variety of reasons, such as differences in protocol, sex, or disease stage [9]. Further, this study utilized a vehicle of 1% sucrose over a period of four months, which may have influenced outcomes on ITT and GTT measures. The utilization of sucrose as a vehicle was based on protocols utilizing this treatment paradigm, indicating the need for sucrose to make the medication palatable for mouse consumption [32].

Examination of liver tissues from both cohorts demonstrated a significant decline in G6P expression and a reduction in circulating insulin levels for male A $\beta$ PP/PS1 riluzole-treated mice. APP<sup>NL-F/NL-F</sup> male mice exhibited increased G6P expression, coinciding with improved glucose tolerance with riluzole treatment. C57BL/6 riluzole-treated males had reduced insulin and glucokinase levels alongside improved glucose tolerance. No significant differences were observed in liver glycogen or serum adiponectin across all genotypes. These findings indicate that changes in G6P expression are independent of circulating insulin and adiponectin and may point to possible alterations to pathways involved in glucose homeostasis and glutamatergic neurotransmission, such as cAMP and CREB signaling. These factors could mediate the observed divergence between genotypes as the expression of several key factors in this signaling pathway are impacted by  $\beta$ -site APP-cleaving enzyme 1 mutations and APP overexpression [58–60].

Riluzole-treated female C57BL/6 mice displayed improved peripheral insulin sensitivity following cessation of treatment, while no significant effects were observed in A $\beta$ PP/PS1 or APP<sup>NL-F/NL-F</sup> female mice. As no treatment effects were observed for serum insulin and adiponectin or target hepatic glucose homeostasis factors for C57BL/6 female mice, the mechanism of this improvement remains uncertain. Further, opposing results observed for glucose tolerance and G6Pase expression in riluzole-treated female APP<sup>NL-F/NL-F</sup> mice support possible hor-

monal interference in riluzole-mediated effects on glucose factors and homeostasis [61].

#### *No off-treatment impact on metabolic tolerance across all genotypes*

At 6-months post-treatment, findings from 12-month-old male and female mice indicate no off-treatment improvement of peripheral insulin and glucose tolerance with riluzole treatment. Sex-dependent treatment effects were observed for the expression of glucokinase, GLUT2, and G6Pase. Yet, these alterations failed to confer an effect on insulin sensitivity and glucose tolerance. The reduction in insulin concentration previously observed in riluzole-treated A $\beta$ PP/PS1 males appeared again post-treatment, now alongside elevated glucokinase and G6Pase expression. These findings indicate that the alterations to glucose factors previously observed were an on-treatment effect that may have shifted with time away from treatment. Collectively, data support on- and off-treatment effects on peripheral glucose tolerance and homeostasis that are dependent on both genotype and sex.

#### *Potentiation of spatial cognition in male riluzole-treated control mice*

Examination of spatial learning and long-term memory immediately following cessation of treatment indicated increased platform entries for riluzole-treated C57BL/6 male mice compared to genotype-matched vehicle-treated mice but showed no significant differences for A $\beta$ PP/PS1 or APP<sup>NL-F/NL-F</sup> male mice. Of note, the only genotype difference observed at this time point was the singular absence of selective searching behavior in A $\beta$ PP/PS1 mice. This may indicate that the males for both AD models had yet to show cognitive deficits at this time point, consistent with previous work from our laboratory utilizing A $\beta$ PP/PS1 males [7] and studies from other laboratories on APP<sup>NL-F/NL-F</sup> mice [42, 62]. A $\beta$ PP/PS1 female mice showed improved spatial learning with rilu-

Fig. 6. Prodromal riluzole treatment improves long-term spatial cognition in male AD mice at 12 months of age. A-C) Spatial learning performance measured by cumulative distance from the platform area. D, E) Platform entries and cumulative distance from the platform during the probe challenge, respectively. F) Analysis of probe challenge quadrant occupancy with percent time. G) Track plots of each genotype and treatment group during the probe challenge. H) ELISA quantification of soluble A $\beta$ <sub>42</sub> levels in the hippocampus. I-K) RT-PCR analysis in hippocampal tissue. Learning trials two-way repeated measures ANOVA, Sidak ( $n = 15-20$ ); probe challenge, RT-PCR ( $n = 6-10$ ), and ELISA analysis ( $n = 5-6$ ) within-genotype unpaired  $t$ -test; Quadrant occupancy one-way ANOVA, Dunnett's (H),  $*p < 0.05$ ,  $**p < 0.01$ ,  $***p < 0.001$ ,  $****p < 0.0001$ .

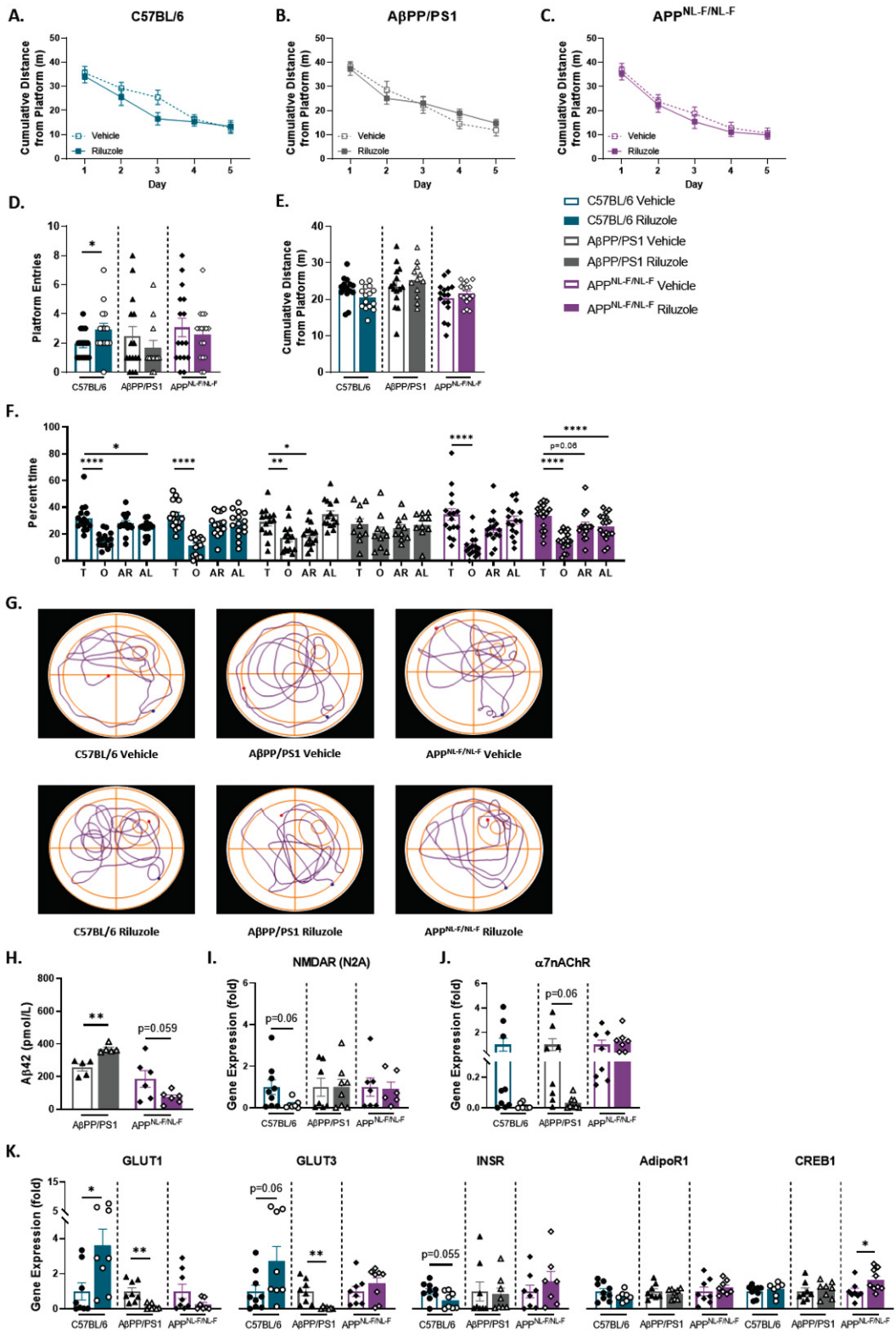


Fig. 7. (Continued)

zole treatment, while APP<sup>NL-F/NL-F</sup> and C57BL/6 female mice did not exhibit any treatment effects. All vehicle-treated female groups at the 6-month time point lacked selective searching behavior during the probe challenge, only showing a modest improvement in preference for the target quadrant with riluzole treatment. However, the discrepancy in spatial learning between female A $\beta$ PP/PS1 treatment groups limited the evaluation of long-term spatial memory. Sex differences observed in MWM performance are in line with previous literature indicating a male advantage to spatial navigation tasks [63].

Riluzole showed an on-treatment reduction in hippocampal  $\alpha$ 7nAChR in male C57BL/6 mice alone, potentially a result of riluzole-mediated excitation inhibition at this time point. An impact was also seen on several factors involved in glucose uptake and homeostasis. GLUT3, AdipoR1, and CREB1 were significantly elevated in riluzole-treated C57BL/6 male mice and reduced in riluzole-treated A $\beta$ PP/PS1 males—who also saw a reduction in GLUT1 expression. In particular, the reduction in GLUT3 expression contrasts previous riluzole research, indicating increased translocation of GLUT3 to the plasma membrane and increased neuronal glucose uptake and utilization [37]. It is possible that the introduction of a pathological amyloidogenic environment overrode the previously observed effects of riluzole. As the plasma membrane in particular was not examined in this study, any impact on the translocation of GLUT3 remains unclear. Notably, as reduced serum insulin was observed for both C57BL/6 and A $\beta$ PP/PS1 males at this time point, this may support that the disparity in glucose transporter expression is independent of peripheral serum findings as both GLUT1 and GLUT3 are insulin-independent. APP<sup>NL-F/NL-F</sup> males exhibited significantly increased INSR and CREB1 expression with riluzole treatment, while no differences were observed in glucose transport. No differences were observed for this model in serum insulin, again supporting that this is a localized hippocampal impact on INSR expression. As INSR

and AdipoR1 are two primary modulators of glucose homeostasis, it follows that CREB1 and glucose transporter expression mirrors the results observed for these respective genes. Additionally, INSR and AdipoR1 are impacted by glutamatergic neurotransmission, providing one potential avenue by which riluzole indirectly impacts central glucose homeostasis [64, 65].

Female C57BL/6 mice at 6 months of age demonstrated elevated AdipoR1 and CREB1 and decreased  $\alpha$ 7nAChR with riluzole treatment—similar to their genotype-matched male counterparts, indicating a sex-independent phenomenon in C57BL/6 mice. A $\beta$ PP/PS1 female mice showed upregulation of INSR expression that was not observed in genotype-matched male mice with riluzole treatment. The upregulation of INSR in riluzole-treated A $\beta$ PP/PS1 female mice also aligns with the observed improvement in spatial learning at this time point. Riluzole-treated APP<sup>NL-F/NL-F</sup> females displayed decreased NMDAR2A and increased GLUT3 expression, unlike their genotype-matched male counterparts. The collective observed sex differences in these findings may result from several factors. Namely, the differences in serum insulin observed in A $\beta$ PP/PS1 and C57BL/6 males were not apparent in genotype-matched female mice. As riluzole-treated C57BL/6 female mice diverged less from treatment-matched C57BL/6 males, these findings could also implicate sex differences in disease pathology as exerting an effect on the disparity of results observed rather than solely a sex-dependent response to riluzole treatment.

#### *Off-treatment effects on spatial navigation and soluble amyloid in AD mice*

At 6 months post-treatment, riluzole-treated male APP<sup>NL-F/NL-F</sup> mice displayed increased platform entries and selective searching behavior compared to vehicle-treated genotype-matched mice. Selective searching behavior was absent in vehicle-treated APP<sup>NL-F/NL-F</sup> male mice, providing further evidence of improved spatial long-term memory in

Fig. 7. Off-treatment changes to spatial cognition in riluzole-treated female C57BL/6 mice at 12 months of age. A-C) Cumulative distance from the platform area throughout the spatial learning trials. D-F) Probe challenge measures include: platform entries (D), cumulative distance from platform (E), and quadrant occupancy (F). G) Track plots of each genotype and treatment group during the probe challenge. H) ELISA quantification of soluble A $\beta$ <sub>42</sub> levels in the hippocampus. I-K) RT-PCR analysis in hippocampal tissue. Learning trials two-way repeated measures ANOVA, Sidak ( $n = 12-19$ ); probe challenge, RT-PCR ( $n = 6-10$ ), and ELISA analysis ( $n = 5-6$ ) within-genotype unpaired  $t$ -test; Quadrant occupancy one-way ANOVA, Dunnett's (H), \* $p < 0.05$ , \*\* $p < 0.01$ , \*\*\* $p < 0.001$ , \*\*\*\* $p < 0.0001$ .

this mouse model. While vehicle-treated male APP<sup>NL-F/NL-F</sup> mice did not differ from vehicle-treated C57BL/6 males, previous studies utilizing various behavioral tasks have observed cognitive deficits around 12–18 months of age [13, 42, 43]. Improvement in long-term spatial memory for riluzole-treated male APP<sup>NL-F/NL-F</sup> mice aligns with RT-PCR findings of on-treatment elevation in INSR expression and on- and off-treatment increase in CREB1 expression, factors previously shown to improve spatial cognition [66].

Riluzole-treated A $\beta$ PP/PS1 male mice showed closer proximity to the immediate platform area at 12 months old, similar to findings previously reported by our laboratory [32]. However, A $\beta$ PP/PS1 males continued to show a lack of selective searching in either treatment group. Further, improvements in long-term spatial memory were observed on different MWM measures between our two AD models. It is possible that a divergence in swim strategy or wayfinding occurred between these models, as these differences would have an impact on which parameters would detect changes in performance. As an improvement for A $\beta$ PP/PS1 males was observed in the proximity to the platform, the effect observed may be tied to executive function and problem-solving rather than long-term memory. Hippocampal RT-PCR findings in A $\beta$ PP/PS1 males would indicate that this improvement occurs through a separate pathway than INSR and would require further examination of synaptic receptors outside of NMDAR2A and  $\alpha$ 7nAChR to pinpoint possible points of impact with riluzole treatment. As well, quantification of soluble A $\beta$ <sub>42</sub> levels in the hippocampus yielded no significant difference for AD male mice on- or off-treatment, in contrast to previously reported findings in 5XFAD male mice [30]. The reasons for these discrepancies and potential insights into select amyloid mutations on wayfinding and responsiveness to glutamatergic modulation should be investigated in future studies.

Notably, male C57BL/6 mice exhibited loss of selective searching behavior with riluzole treatment, indicating that prior improvements in long-term spatial memory performance were limited to an on-treatment effect. Data from 6 months post-treatment in male AD mice may indicate that riluzole's potential off-treatment cognitive benefits are confined to pathological conditions. Conversely, female C57BL/6 mice displayed increased platform entries with riluzole treatment compared to matched vehicle-treated C57BL/6s at 6 months post-treatment only. Results from C57BL/6 female mice may highlight a sex-

dependent shift in glutamatergic neurotransmission with age in C57BL/6 mice, such that glutamate modulation at an early age provided procognitive effects at different time points and warrants further study. Riluzole-treated APP<sup>NL-F/NL-F</sup> female mice displayed selective searching behavior, while A $\beta$ PP/PS1 females lost all preference for the target quadrant with riluzole treatment. Subsequent quantification of soluble A $\beta$ <sub>42</sub> in the hippocampus revealed increased A $\beta$ <sub>42</sub> concentration in A $\beta$ PP/PS1 female mice with riluzole treatment that likely contributed to the decline in spatial memory performance. Conversely, a decrease in A $\beta$ <sub>42</sub> concentration was observed for riluzole-treated APP<sup>NL-F/NL-F</sup> female mice, congruent with the observed improvement in spatial cognition. Future studies should investigate impacts on the A $\beta$ <sub>40:42</sub> ratio and plaque load in the hippocampus with riluzole treatment in A $\beta$ PP/PS1 and APP<sup>NL-F/NL-F</sup> mice to clarify the mechanism by which this division in amyloid pathology occurs.

#### *Off-treatment alterations to key factors in glutamate and glucose homeostasis*

At 6 months post-treatment, male C57BL/6 mice continued to display reduced  $\alpha$ 7nAChR expression, indicating an on- and off-treatment impact on an important mediator of presynaptic glutamate release. A $\beta$ PP/PS1 male mice also showed a reduction in  $\alpha$ 7nAChR with riluzole treatment, while APP<sup>NL-F/NL-F</sup> riluzole-treated males showed an increase. We previously reported that  $\alpha$ 7nAChR density in the hippocampus was not affected by riluzole treatment in 12-month-old A $\beta$ PP/PS1 mice, indicating that riluzole-mediated glutamatergic alterations are independent of A $\beta$ - $\alpha$ 7nAChR glutamate release. [32]. However, our previous study did not examine riluzole treatment in C57BL/6 and APP<sup>NL-F/NL-F</sup> males, and the impact on hippocampal  $\alpha$ 7nAChR surface density in light of our current PCR findings remains uncertain.

Opposing results to that reported on-treatment for C57BL/6 males were observed for GLUT3, AdipoR1, and CREB1, in addition to reductions in GLUT1 and INSR. Data may support that age and time away from treatment led to a downregulation of glucose factors for C57BL/6 males. A $\beta$ PP/PS1 males continued to display reduced GLUT3 and CREB1 expression, now alongside a significant reduction in INSR expression. These findings may be partly influenced by the reduction in serum insulin observed in A $\beta$ PP/PS1 males at this time. Elevated CREB1

in riluzole-treated APP<sup>NL-F/NL-F</sup> males was also observed at this time point, similar to that reported while on treatment, pointing to a prolonged upregulation of CREB1 in this model that may contribute in part to improved cognitive outcomes.

Riluzole-treated C57BL/6 female mice exhibited elevated GLUT1 and GLUT3 and decreased INSR expression at 6 months post-treatment. As both glucose transporters are insulin-independent, it follows that alterations in INSR expression may not mirror changes in GLUT1 expression. These findings also contrast that observed for glucose transport expression in respective male C57BL/6 mice, possibly indicating a hormonally influenced outcome with age and time away from treatment in C57BL/6 mice that is independent of insulin. Results from A $\beta$ PP/PS1 female mice indicated decreased GLUT1 and GLUT3 expression with riluzole treatment—a selectively off-treatment effect. As elevated soluble A $\beta$ <sub>42</sub> was observed at this time point in the hippocampus, it is possible that the downregulation of glucose transporter expression was amyloid-mediated with riluzole treatment [67]. APP<sup>NL-F/NL-F</sup> female mice showed elevated CREB1 expression with riluzole treatment, an off-treatment effect seemingly independent of INSR and AdipoR1 and similar to that observed in their riluzole-treated male counterparts. As CREB1 expression is vulnerable to influences from many different pathways, including glutamatergic neurotransmission, further investigation would be required to discern the direct cause of this increase. Gene expression results from hippocampal RT-PCR studies indicate sex-dependent changes in important factors for glutamate and glucose homeostasis with riluzole treatment that have the potential to impact cognition both on- and off-treatment.

Collectively, these findings support sex and genotype differences in response to riluzole treatment that may impact cognitive outcomes. An effective intervention strategy that utilizes glutamatergic modulation requires accurate timing of treatment with hippocampal glutamate dynamics that shift with age and disease progression and are specific to each genotype and sex. Targeting of the glutamatergic system through riluzole did impact glucose homeostasis in the hippocampus and periphery but elicited a stronger response from male mice and warrants further investigation as to the lack of responsiveness in female AD mice. Thus, manipulation of the interconnected pathological relationship between glutamate and glucose homeostasis and amyloid pathology requires a

nanced and tailored strategy to ameliorate cognitive decline effectively.

## ACKNOWLEDGMENTS

The authors have no acknowledgments to report.

## FUNDING

This work was supported by the National Institutes of Health (R01 AG057767, R01 AG061937, R21 AG062985), the Dale and Deborah Smith Center for Alzheimer's Research and Treatment, and the Kenneth Stark Endowment.

## CONFLICT OF INTEREST

E. Hascup is an Editorial Board Member of this journal but was not involved in the peer-review process nor had access to any information regarding its peer-review. The authors have no other conflict of interest to report.

## DATA AVAILABILITY

The data supporting the findings of this study are available on request from the corresponding author.

## SUPPLEMENTARY MATERIAL

The supplementary material is available in the electronic version of this article: <https://dx.doi.org/10.3233/JAD-221245>.

## REFERENCES

- [1] Alzheimer's Association (2022) 2022 Alzheimer's disease facts and figures. *Alzheimers Dement* **18**, 700-789.
- [2] Heron M (2021) Deaths: Leading causes for 2019. *Natl Vital Stat Reports* **70**, 1-113.
- [3] Edwards GA, Gamez N, Escobedo G, Calderon O, Moreno-Gonzalez I (2019) Modifiable risk factors for Alzheimer's disease. *Front Aging Neurosci* **11**, 146.
- [4] Barbagallo M, Dominguez LJ (2014) Type 2 diabetes mellitus and Alzheimer's disease. *World J Diabetes* **5**, 889.
- [5] Alexander GC, Emerson S, Kesselheim AS (2021) Evaluation of Aducanumab for Alzheimer disease: Scientific evidence and regulatory review involving efficacy, safety, and futility. *JAMA* **325**, 1717-1718.
- [6] Jack CR, Holtzman DM (2013) Biomarker modeling of Alzheimer's disease. *Neuron* **80**, 1347-1358.
- [7] Hascup KN, Findley CA, Sime LN, Hascup ER (2020) Hippocampal alterations in glutamatergic signaling during amyloid progression in A $\beta$ PP/PS1 mice. *Sci Rep* **10**, 14503.

- [8] Pedrós I, Petrov D, Allgaier M, Sureda F, Barroso E, Beas-Zarate C, Auladell C, Pallàs M, Vázquez-Carrera M, Casadesús G, Folch J, Camins A (2014) Early alterations in energy metabolism in the hippocampus of APP<sup>sw</sup>/PS1<sup>de9</sup> mouse model of Alzheimer's disease. *Biochim Biophys Acta* **1842**, 1556-1566.
- [9] Griffith CM, Eid T, Rose GM, Patrylo PR (2018) Evidence for altered insulin receptor signaling in Alzheimer's disease. *Neuropharmacology* **136**, 202-215.
- [10] Connolly NMC, Theurey P, Pizzo P (2019) Glucose dysregulation in pre-clinical Alzheimer's disease. *Aging (Albany NY)* **11**, 5296-5297.
- [11] Cox MF, Hascup ER, Bartke A, Hascup KN (2022) Friend or foe? Defining the role of glutamate in aging and Alzheimer's disease. *Front Aging* **3**, 65.
- [12] Hascup ER, Broderick SO, Russell MK, Fang Y, Bartke A, Boger HA, Hascup KN (2019) Diet-induced insulin resistance elevates hippocampal glutamate as well as VGLUT1 and GFAP expression in A $\beta$ PP/PS1 mice. *J Neurochem* **148**, 219-237.
- [13] Mazzei G, Ikegami R, Abolhassani N, Haruyama N, Sakumi K, Saito T, Saido TC, Nakabeppu Y (2021) A high-fat diet exacerbates the Alzheimer's disease pathology in the hippocampus of the App<sup>NL-F/NL-F</sup> knock-in mouse model. *Aging Cell* **20**, e13429.
- [14] Valladolid-Acebes I, Merino B, Principato A, Fole A, Barbas C, Lorenzo MP, García A, Del Olmo N, Ruiz-Gayo M, Cano V (2012) High-fat diets induce changes in hippocampal glutamate metabolism and neurotransmission. *Am J Physiol Metab* **302**, E396-E402.
- [15] Stefani A, Spadoni F, Bernardi G (1997) Differential inhibition by riluzole, lamotrigine, and phenytoin of sodium and calcium currents in cortical neurons: Implications for neuroprotective strategies. *Exp Neurol* **147**, 115-122.
- [16] Zona C, Siniscalchi A, Mercuri N, Bernardi G (1998) Riluzole interacts with voltage-activated sodium and potassium currents in cultured rat cortical neurons. *Neuroscience* **85**, 931-938.
- [17] Spadoni F, Hainsworth AH, Mercuri NB, Caputi L, Martella G, Lavaroni F, Bernardi G, Stefani A (2002) Lamotrigine derivatives and riluzole inhibit INa,P in cortical neurons. *Neuroreport* **13**, 1167-1170.
- [18] Cheah BC, Vucic S, Krishnan A, Kiernan MC (2010) Riluzole, neuroprotection and amyotrophic lateral sclerosis. *Curr Med Chem* **17**, 1942-1959.
- [19] Bellingham MC (2011) A review of the neural mechanisms of action and clinical efficiency of riluzole in treating amyotrophic lateral sclerosis: What have we learned in the last decade? *CNS Neurosci Ther* **17**, 4-31.
- [20] Cao Y-J, Dreixler JC, Couey JJ, Houamed KM (2002) Modulation of recombinant and native neuronal SK channels by the neuroprotective drug riluzole. *Eur J Pharmacol* **449**, 47-54.
- [21] Bellingham MC, Walmsley B (1999) A novel presynaptic inhibitory mechanism underlies paired pulse depression at a fast central synapse. *Neuron* **23**, 159-170.
- [22] Ireland MF, Noakes PG, Bellingham MC (2004) P2X7-like receptor subunits enhance excitatory synaptic transmission at central synapses by presynaptic mechanisms. *Neuroscience* **128**, 269-280.
- [23] Frizzo ME dos S, Dall'Onder LP, Dalcin KB, Souza DO (2004) Riluzole enhances glutamate uptake in rat astrocyte cultures. *Cell Mol Neurobiol* **24**, 123-8.
- [24] Fumagalli E, Funicello M, Rauen T, Gobbi M, Mennini T (2008) Riluzole enhances the activity of glutamate transporters GLAST, GLT1 and EAAC1. *Eur J Pharmacol* **578**, 171-176.
- [25] Carbone M, Duty S, Rattray M (2012) Riluzole elevates GLT-1 activity and levels in striatal astrocytes. *Neurochem Int* **60**, 31-38.
- [26] Hunsberger HC, Weitzner DS, Rudy CC, Hickman JE, Libell EM, Speer RR, Gerhardt GA, Reed MN (2015) Riluzole rescues glutamate alterations, cognitive deficits, and tau pathology associated with P301L tau expression. *J Neurochem* **135**, 381-394.
- [27] Deng Y, Xu Z, Xu B, Tian Y, Xin X, Deng X, Gao J (2009) The protective effect of riluzole on manganese caused disruption of glutamate-glutamine cycle in rats. *Brain Res* **1289**, 106-117.
- [28] Brothers HM, Bardou I, Hopp SC, Kaercher RM, Corona AW, Fenn AM, Godbout JP, Wenk GL (2013) Riluzole partially rescues age-associated, but not LPS-induced, loss of glutamate transporters and spatial memory. *J Neuroimmune Pharmacol* **8**, 1098-1105.
- [29] Mokhtari Z, Baluchnejadmojarad T, Nikbakht F, Mansouri M, Roghani M (2017) Riluzole ameliorates learning and memory deficits in A $\beta$ 25-35-induced rat model of Alzheimer's disease and is independent of cholinergic activation. *Biomed Pharmacother* **87**, 135-144.
- [30] Okamoto M, Gray JD, Larson CS, Kazim SF, Soya H, McEwen BS, Pereira AC (2018) Riluzole reduces amyloid beta pathology, improves memory, and restores gene expression changes in a transgenic mouse model of early-onset Alzheimer's disease. *Transl Psychiatry* **8**, 153.
- [31] Lesuis SL, Kaplick PM, Lucassen PJ, Krugers HJ (2019) Treatment with the glutamate modulator riluzole prevents early life stress-induced cognitive deficits and impairments in synaptic plasticity in APP<sup>sw</sup>/PS1<sup>de9</sup> mice. *Neuropharmacology* **150**, 175-183.
- [32] Hascup KN, Findley CA, Britz J, Esperant-Hilaire N, Broderick SO, Delfino K, Tischkau S, Bartke A, Hascup ER (2021) Riluzole attenuates glutamatergic tone and cognitive decline in A $\beta$ PP/PS1 mice. *J Neurochem* **156**, 513-523.
- [33] Hascup KN, Lynn MK, Fitzgerald PJ, Randall S, Kopchick J, Boger HA, Bartke A, Hascup ER (2016) Enhanced cognition and hypoglutamatergic signaling in a growth hormone receptor knockout mouse model of successful aging. *J Gerontol A Biol Sci Med Sci* **72**, 329-337.
- [34] Knight EM, Martins IVA, Gümüşgöz S, Allan SM, Lawrence CB (2014) High-fat diet-induced memory impairment in triple-transgenic Alzheimer's disease (3xTgAD) mice is independent of changes in amyloid and tau pathology. *Neurobiol Aging* **35**, 1821-1832.
- [35] Sadowski M, Pankiewicz J, Scholtzova H, Ji Y, Quartermain D, Jensen CH, Duff K, Nixon RA, Gruen RJ, Wisniewski T (2004) Amyloid- $\beta$  deposition is associated with decreased hippocampal glucose metabolism and spatial memory impairment in APP/PS1 mice. *J Neuropathol Exp Neurol* **63**, 418-428.
- [36] Matthews DC, Mao X, Dowd K, Tsakanikas D, Jiang CS, Meuser C, Andrews RD, Lukic AS, Lee J, Hampilos N, Shafiq N, Sano M, David Mozley P, Fillit H, McEwen BS, Shungu DC, Pereira AC (2021) Riluzole, a glutamate modulator, slows cerebral glucose metabolism decline in patients with Alzheimer's disease. *Brain* **144**, 3742-3755.
- [37] Daniel B, Green O, Viskind O, Gruzman A (2013) Riluzole increases the rate of glucose transport in L6 myotubes and NSC-34 motor neuron-like cells via AMPK pathway activation. *Amyotroph Lateral Scler Front Degener* **14**, 434-443.

- [38] Chowdhury GMI, Banasr M, de Graaf RA, Rothman DL, Behar KL, Sanacora G (2008) Chronic riluzole treatment increases glucose metabolism in rat prefrontal cortex and hippocampus. *J Cereb Blood Flow Metab* **28**, 1892-1897.
- [39] Macotela Y, Boucher J, Tran TT, Kahn CR (2009) Sex and depot differences in adipocyte insulin sensitivity and glucose metabolism. *Diabetes* **58**, 803-12.
- [40] Cnop M, Havel PJ, Utzschneider KM, Carr DB, Sinha MK, Boyko EJ, Retzlaff BM, Knopp RH, Brunzell JD, Kahn SE (2003) Relationship of adiponectin to body fat distribution, insulin sensitivity and plasma lipoproteins: Evidence for independent roles of age and sex. *Diabetologia* **46**, 459-469.
- [41] Knight EM, Ruiz HH, Kim SH, Harte JC, Hsieh W, Glabe C, Klein WL, Attie AD, Buettner C, Ehrlich ME, Gandy S (2016) Unexpected partial correction of metabolic and behavioral phenotypes of Alzheimer's APP/PSEN1 mice by gene targeting of diabetes/Alzheimer's-related Sorcs1. *Acta Neuropathol Commun* **4**, 16.
- [42] Saito T, Matsuba Y, Mihira N, Takano J, Nilsson P, Itohara S, Iwata N, Saido TC (2014) Single App knock-in mouse models of Alzheimer's disease. *Nat Neurosci* **17**, 661-663.
- [43] Masuda A, Kobayashi Y, Kogo N, Saito T, Saido TC, Itohara S (2016) Cognitive deficits in single App knock-in mouse models. *Neurobiol Learn Mem* **135**, 73-82.
- [44] Hascup ER, Sime LN, Peck MR, Hascup KN (2022) Amyloid- $\beta$ 42 stimulated hippocampal lactate release is coupled to glutamate uptake. *Sci Rep* **12**, 2775.
- [45] Hascup KN, Britz J, Findley CA, Tischkau S, Hascup ER (2019) LY379268 does not have long-term procognitive effects nor attenuate glutamatergic signaling in A $\beta$ PP/PS1 mice. *J Alzheimers Dis* **68**, 1193-1209.
- [46] Hardingham GE, Bading H (2010) Synaptic versus extrasynaptic NMDA receptor signalling: Implications for neurodegenerative disorders. *Nat Rev Neurosci* **11**, 682-696.
- [47] Hascup KN, Hascup ER (2016) Soluble Amyloid- $\beta$ 42 stimulates glutamate release through activation of the  $\alpha$ 7 nicotinic acetylcholine receptor. *J Alzheimers Dis* **53**, 337-347.
- [48] Wang HY, Lee DHS, Davis CB, Shank RP (2000) Amyloid peptide A $\beta$ 1-42 binds selectively and with picomolar affinity to  $\alpha$ 7 nicotinic acetylcholine receptors. *J Neurochem* **75**, 1155-1161.
- [49] Li S, Nai Q, Lipina TV, Roder JC, Liu F (2013)  $\alpha$ 7NACHR/NMDAR coupling affects NMDAR function and object recognition. *Mol Brain* **6**, 58.
- [50] Jiang A, Su P, Li S, Wong AHC, Liu F (2021) Disrupting the  $\alpha$ 7nAChR-NR2A protein complex exerts antidepressant-like effects. *Mol Brain* **14**, 107.
- [51] Olney JW, Wozniak DF, Farber NB (1997) Excitotoxic neurodegeneration in Alzheimer disease. New hypothesis and new therapeutic strategies. *Arch Neurol* **54**, 1234-1240.
- [52] Parsons CG, Stöfler A, Danysz W (2007) Memantine: A NMDA receptor antagonist that improves memory by restoration of homeostasis in the glutamatergic system - too little activation is bad, too much is even worse. *Neuropharmacology* **53**, 699-723.
- [53] Macklin L, Griffith CM, Cai Y, Rose GM, Yan XX, Patrylo PR (2017) Glucose tolerance and insulin sensitivity are impaired in APP/PS1 transgenic mice prior to amyloid plaque pathogenesis and cognitive decline. *Exp Gerontol* **88**, 9-18.
- [54] Zhang Y, Zhou B, Zhang F, Wu J, Hu Y, Liu Y, Zhai Q (2012) Amyloid- $\beta$  induces hepatic insulin resistance by activating JAK2/STAT3/SOCS-1 signaling pathway. *Diabetes* **61**, 1434-1443.
- [55] Clarke JR, Lyra e Silva NM, Figueiredo CP, Frozza RL, Ledo JH, Beckman D, Katashima CK, Razolli D, Carvalho BM, Frazão R, Silveira MA, Ribeiro FC, Bomfim TR, Neves FS, Klein WL, Medeiros R, LaFerla FM, Carvalho JB, Saad MJ, Munoz DP, Velloso LA, Ferreira ST, De Felice FG (2015) Alzheimer-associated A $\beta$  oligomers impact the central nervous system to induce peripheral metabolic deregulation. *EMBO Mol Med* **7**, 190-210.
- [56] Mody N, Agouni A, McIlroy GD, Platt B, Delibegovic M (2011) Susceptibility to diet-induced obesity and glucose intolerance in the APPSWE/PSEN1A246E mouse model of Alzheimer's disease is associated with increased brain levels of protein tyrosine phosphatase 1B (PTP1B) and retinobinding protein 4 (RBP4), and basal phosphorylation of S6 ribosomal protein. *Diabetologia* **54**, 2143-2151.
- [57] Ruiz HH, Chi T, Shin AC, Lindtner C, Hsieh W, Ehrlich M, Gandy S, Buettner C (2016) Increased susceptibility to metabolic dysregulation in a mouse model of Alzheimer's disease is associated with impaired hypothalamic insulin signaling and elevated BCAA levels. *Alzheimers Dement* **12**, 851-861.
- [58] Lahiri D, Ge Y-W, Rogers J, Sambamurti K, Greig N, Maloney B (2006) Taking down the unindicted co-conspirators of amyloid beta-peptide mediated neuronal death: Shared gene regulation of BACE1 and APP genes interacting with CREB, Fe65 and YY1 transcription factors. *Curr Alzheimer Res* **3**, 475-483.
- [59] Pugazhenthis S, Wang M, Pham S, Sze CI, Eckman CB (2011) Downregulation of CREB expression in Alzheimer's brain and in A $\beta$ -treated rat hippocampal neurons. *Mol Neurodegener* **6**, 60.
- [60] Chen Y, Huang X, Zhang YW, Rockenstein E, Bu G, Golde TE, Masliah E, Xu H (2012) Alzheimer's  $\beta$ -secretase (BACE1) regulates the cAMP/PKA/CREB pathway independently of  $\beta$ -amyloid. *J Neurosci* **32**, 11390-11395.
- [61] Richard JE, Anderberg RH, López-Ferreras L, Olandersson K, Skibicka KP (2016) Sex and estrogens alter the action of glucagon-like peptide-1 on reward. *Biol Sex Differ* **7**, 6.
- [62] Britz J, Ojo E, Dhukhwa A, Saito T, Saido TC, Hascup ER, Hascup KN, Tischkau SA (2022) Assessing sex-specific circadian, metabolic, and cognitive phenotypes in the A $\beta$ PP/PS1 and APPNL-F/NL-F models of Alzheimer's disease. *J Alzheimers Dis* **85**, 1077-1093.
- [63] Andreano JM, Cahill L (2009) Sex influences on the neurobiology of learning and memory. *Learn Mem* **16**, 248-266.
- [64] Ettchetto M, Petrov D, Pedros I, Alva N, Carbonell T, Beas-Zarate C, Pallas M, Auladell C, Folch J, Camins A (2016) Evaluation of neuropathological effects of a high-fat diet in a presymptomatic Alzheimer's disease stage in APP/PS1 mice. *J Alzheimers Dis* **54**, 233-251.
- [65] Liu B, Liu J, Wang J, Sun F, Jiang S, Hu F, Wang D, Liu D, Liu C, Yan H (2019) Adiponectin protects against cerebral ischemic injury through AdipoR1/AMPK pathways. *Front Pharmacol* **10**, 597.
- [66] Ferreira LSS, Fernandes CS, Vieira MNN, De Felice FG (2018) Insulin resistance in Alzheimer's disease. *Front Neurosci* **12**, 830.
- [67] Ding F, Yao J, Rettberg JR, Chen S, Brinton RD (2013) Early decline in glucose transport and metabolism precedes shift to ketogenic system in female aging and Alzheimer's mouse brain: Implication for bioenergetic intervention. *PLoS One* **8**, e79977.